F. Soto, G. Marques, L. Soto-Izquierdo, E. Torres-Jiménez, S. Quaglia, F. Guerrero-Villar, R. Dorado-Vicente, J. Abdalla (2021) Performance and regulated emissions of a medium-duty diesel engine fueled with biofuels from sugarcane over the European steady cycle (ESC),Fuel,Volume 292,120326,ISSN 0016-2361, https://doi.org/10.1016/j.fuel.2021.120326

Performance and Regulated Emissions of a Medium-Duty Diesel Engine Fueled with Biofuels from Sugarcane over the European Steady Cycle (ESC)

Felipe Soto[a], Gian Marques[b], Lian Soto Izquierdo[b], Eloísa Torres-Jiménez[c,*], Saulo Quaglia[a], Francisca Guerrero-Villar[c], Rubén Dorado-Vicente[c], Jordana Abdalla[a]

[a] *Universidade Federal de São João del-Rei, Praça Frei Orlando, 170, São João del-Rei-Minas Gerais, CEP: 36307-352, Brazil*

[b] *Research associate in the project "Potencial energético e ambiental de um novo combustível e biocombustível em motores diesel" Universidade Federal de São João del-Rei, Praça Frei Orlando, 170, São João del-Rei-Minas Gerais, CEP: 36307-352, Brazil*

[c] *Universidad de Jaén, Department of Mechanical and Mining Engineering, Campus las Lagunillas s/n, A3, 23071, Jaén, Spain*

*Corresponding author: etorres@ujaen.es (E. Torres-Jiménez)

Keywords:

European Steady Cycle; Sugarcane biodiesel; Sugarcane diesel-farnesane; Oxidation inhibition; Diesel Oxidation Catalyst; Engine exhaust emissions

Abstract

The use of diesel-farnesane and sugarcane biodiesel is showing significant potential for reducing harmful emissions from Brazilian road transport. Both biofuels are obtained from sugarcane through synthetic biology that requires fermentation. The present work studies the effect of the sugarcane biofuels, compared to regular diesel fuel, on the performance and emissions of a modern medium-duty diesel engine following the European Steady Cycle (ESC) test procedure. Diesel-farnesane showed the lowest particulate matter (PM) specific emissions. Specific nitrogen oxides (NOx) emissions from diesel fuel were above the standard limit, while sugarcane biodiesel produced the lowest emissions. All tested fuels produced specific carbon monoxide (CO) emissions below the standard limit, but the biofuels showed higher values than the reference fuel. Sugarcane biodiesel showed an inhibition effect on the oxidation process at

the Diesel Oxidation Catalyst (DOC), leading to the highest specific CO emissions after the DOC. Specific total hydrocarbons (THC) emissions were well below the standard limits for all tested fuels. Concerning the regulated emissions for diesel engines (g/h), the use of sugarcane biodiesel led to PM and NOx reductions of 32.4% and 37.3%, while diesel-farnesane led to 41.7% and 6.08% reductions, respectively. These notable reductions in harmful emissions support the application of sugarcane biofuels to road transport.

Nomenclature

$(A/F)_{st}$ - Stoichiometric air-fuel ratio

Bsfc - brake specific fuel consumption

C_{gas} - concentration of the exhaust gas component

CLD - Chemilumines-cence Detector

CN – cetane number

DOC - diesel oxidation catalyst

ec - energy per cycle

ECU - Engine Control Unit

EGR – exhaust gas recirculation

ELR – European Load Response

EPA - United States Environmental Protection Agency

ESC – European Steady Cycle

ETC - European Transient Cycle

Euro V - European emission standards 5

F/A - fuel-air ratio

F30 - 30% sugarcane diesel-farnesane/diesel fuel blend

FID - Flame Ionization Detector

FSN – Filter smoke Number

GTL - gas to liquid

H/C – hydrogen/carbon ratio

HC – hydrocarbon

IRD - Infrared Detector

$k_{h,d}$ - correction factor

LDD - Laser Diode Detector

LHV - Lower heating value

m_f – modes of mass flow

m_{gas} - mass flow emission

N – engine speed

NEDC - New European Driving Cycle

n_{hi} – engine high speed

n_{lo} – engine low speed

P – Power

P_e – mean effective pressure

P_f - engine power

PM – particulate matter

PMD - Paramagnetic Detector

Proconve - Motor Vehicle Air Pollution Control Program

Proconve P7 – phase 7 of Proconve

PT_{mass} – mass flow

QCL - Quantum Cascade Laser

q_{mew} - mass flow of the exhaust gases

REG - Renewable Energy Group

S50 - mineral diesel and 5% biodiesel blend

T – torque

T_g - gas temperature

THC - total hydrocarbons

u_{gas} - density of a determined pollutant/density of the exhaust gases

USA – United States of America

v/v – volume per volume

W_{Fi} - weight factor

WLTC - Worldwide harmonized Light-duty vehicles Test Cycle

Z_i – modes compared

Chemical formula

$C_{15.2}H_{27.3}$* - Diesel S50

$C_{15}H_{32}$ (2,6,10-trimetildodecane) – diesel-farnesane

$C_{16}H_{30}O_2$ – Sugarcane biodiesel

C_2H_2 - acetylene

CH_4 - methane

CO – carbon monoxide

CO_2 – carbon dioxide

N_2O – nitrogen dioxide

NH_3 – ammonia gas

NO – nitrogen oxide

NOx – nitrogen oxides

O_2 - oxygen

Greek symbols

ϕ - fuel-air equivalence ratio

χ - product of thermal efficiency and fuel-air equivalence ratio

η_t - thermal efficiency of the engine

Subscripts

e – effective

f= fuel (S50, Diesel-farnesane, Sugarcane-biodiesel)

Fi – factor of the mode

g –gas (NOx, CO, THC)

hi - high speed

i – number of modes compared

lo – low speed

mew – measured in the exhaust gas

St – stoichiometric

t – thermal

1. Introduction

The optimization of the design and manufacturing of engines for the usage of biofuels can help to mitigate the environmental problem that arises from the use of fossil fuels. This is a holistic approach that considers both the engine technology and fuel composition. The development of alternative fuels to substitute those derived from petroleum, such as diesel fuel, is an interesting research topic due to its application in the transportation sector. A practical application of alternative fuels requires their study to optimize the management strategies implemented in the Engine Control Unit (ECU).

This work is focused on two biofuels derived from sugarcane that can power a compression ignition engine and, therefore, can substitute for mineral diesel fuel: diesel-farnesane and sugarcane biodiesel, commercially developed by Amyris and the start-up LS9 (the latter acquired by REG Life Sciences in 2014), respectively. Both fuels involve a synthetic biology process that requires fermentation [1]. The fact that these biofuels are considered as promising alternatives to mineral diesel fuel motivates the present study. They are produced exclusively in Brazil by the USA based companies noted above. On the other hand, Brazil is a well-known innovator in the

field of biofuels production and consumption, especially those fuels obtained from sugarcane. Traditionally, this raw material is used to produce bioethanol, which can power a gasoline engine. In particular, since 1931, Brazil uses ethanol as a biofuel, and it is the worldwide leader in sugarcane ethanol production [2]. Many research works have unsuccessfully tried to use ethanol in diesel cycles. Amyris and LS9 have patented a process to obtain diesel fuel substitutes from sugarcane. According to the United States' EPA [3], sugarcane biodiesel offers an 85% reduction in carbon footprint, absence of heavy metals, sulfur, and benzene present in mineral diesel, and had a competitive price of $45-50 per barrel at the time of the EPA's report. The interest in Farnesane has been highlighted by recent studies recommending it as a promising advanced biofuel for aviation and diesel engines due to its low NOx and soot emissions [4]. Even more, Farnesane is more commercially viable than other biofuels because it is already produced in Brazil by Amyris [5].

Sugarcane diesel-farnesane is an iso-paraffin $C_{15}H_{32}$ (2,6,10-trimetildodecane) [6]. This fuel blended with mineral diesel in concentrations from 10% to 30% v/v was used until 2016 by 400 public buses in the city of São Paulo. In Rio de Janeiro, Cachiolo et al. [7] studied the use of diesel-farnesane in urban freight transport.

On the other hand, sugarcane biodiesel results from a fermentation process followed by a methyl transesterification process. The fermentation is driven by genetically modified yeasts, which produces a blend of fatty acids with different structures. Next, the same transesterification process used to produce soybean biodiesel ($C_{18.2}H_{33.4}O_2$) is applied to obtain sugarcane biodiesel: a mixture of unsaturated esters with the molecular structure ($C_{16}H_{30}O_2$) [8]. Note that, while soybean fatty acid is composed of different unsaturated fatty acids, the sugarcane fatty acid is pure and saturated. Hence, the properties of $C_{18.2}H_{33.4}O_2$ and $C_{16}H_{30}O_2$ are different, such as the Cetane number (50.6 vs. 69.9), and the Lower Heating Value (36.8 $MJ \cdot kg^{-1}$ vs. 35.80 $MJ \cdot kg^{-1}$).

There are few published works on the use of diesel-farnesane in engines, and even fewer studies focused on sugarcane biodiesel. In a previous work [9], the authors analyzed the emissions and performance of a medium-duty engine for both fuels over the European Transient Cycle (ETC) with good results. This type of engine must also meet the European Stationary Cycle (ESC), which is analyzed in the present paper, with an emphasis on regulations and procedures related to medium-duty engines. In the opinion of the authors, it is also important to study this class of engines because most of them are diesel engines and, consequently, they can be powered by the new fuels tested.

Authors such as Conconi and Crnkovic [10, 11] studied the thermal degradation of sugarcane diesel-farnesane in environments other than the combustion chamber of a reciprocating engine. They performed thermogravimetric oxidation tests showing that diesel-farnesane has lower oxidation activation energy than mineral diesel fuel and helped to find a correlation between the activation energy and the CO_2 emissions measured during ESC tests. Soto et al. [12] provided an in-depth discussion of the correlation between the activation energy obtained by thermal degradation at atmospheric pressure and engine performance and emissions.

Tests accomplished at atmospheric pressure showed that diesel-farnesane reduces the production of soot precursors [5]. Experimental tests on hydro processed biofuels in a shock-tube revealed a shorter ignition delay time than mineral diesel for temperatures from 650 K to 900 K with an increase of the cetane number (CN) [13, 14]. Gowdagiri et al. [15] reported that the ignition delay is related to changes in the CN. These authors noted that diesel-farnesane causes unexpectedly high CO emissions due to its phase change characteristics, which could lead to high THC emissions as well. These researchers highlighted that diesel-farnesane reduces NOx emissions with respect to the reference diesel fuel and they discussed the relationship between the H/C ratio and NOx emissions. Their results are in good agreement with the work of Cecrle et al. [16], who measured NOx emissions of the same engine fueled by biodiesel.

For a 30% sugarcane diesel-farnesane/diesel fuel blend (F30) tested in an engine at full and at partial loads, either with modification or without modification of ECU, Millo et al. [17] found no significant variations in CO_2 emissions with the recalibration, since the specific fuel consumption and the carbon content remained nearly the same for both fuels. In all cases, F30 showed lower specific CO and THC emissions at low and medium loads, while no significant variations were observed at full load. Without recalibration, the specific NOx emissions of the blend were higher than those of mineral diesel fuel at medium and full load. After recalibration of the ECU to the blend, the emissions were similar. It was noted that there was a significant reduction in soot emissions at medium and full loads for F30. According to these authors, the lack of soot precursors and aromatic hydrocarbons in sugarcane diesel-farnesane promotes this reduction.

Soriano et al. [18] studied a light-duty engine without ECU modification fueled by sugarcane diesel-farnesane, soybean-palm biodiesel, gas to liquid (GTL) fuel and mineral diesel fuel. Five operating modes were tested, identified by an application of a design of experiments methodology [19]. The results highlighted the benefits to THC and PM emissions through the use of all alternative fuels tested, especially diesel-farnesane.

In the present work, two biofuels obtained from sugarcane, biodiesel and diesel-farnesane, are compared with a reference fuel by means of experimental engine tests. The S50, a blend of mineral diesel and 5% biodiesel, is the reference fuel, and it is available at fuel stations across Brazil. The experimental tests are performed in a medium-sized diesel engine used for road transport in Brazil according to the Proconve P7 standard. As part of the program to control air pollution, Brazil developed the Proconve P7 standard that meets the recommendations of Euro V. Studies such as the present one are needed to ensure that the substitution of diesel fuel by new biofuels for road transport in Brazil is safe and beneficial.

The main goal of this work is to determine the influence of the aforementioned biofuels in engine performance, exhaust gas emissions and specific PM emissions without ECU

recalibration. Firstly, it is determined whether the fuels meet the limits specified by the Brazilian regulation that is based on the 13 modes of the ESC procedure. The results obtained are also analyzed to find improved performance when using the biofuels under this testing procedure. It is worth mentioning that to satisfy the Proconve P7 standard, in addition to the ESC test shown in this work, two additional tests are required: the ETC test presented in [9] and the ELR test, which is currently in progress. After this assessment, we extend the analysis to the comparison of fuels. Because misleading conclusions about the emissions can be attained due to differences in the lower heating value (LHV) among the fuels, 12 modes (Z_i) where the three fuels provide the same engine power are analyzed. Finally, the ESC results allowed us to define the toxicity characteristics, which to interesting comparisons of the results for the different operating regimes.

Although sugarcane is widely used as raw material for bioethanol production, the biofuels studied here are still relatively uncommon since they are intended to power a diesel engine. For this reason, this study contributes to a new body of knowledge in the field of biofuels, by analyzing and experimentally testing two biofuels from sugarcane in a diesel engine. The present study expands the knowledge about them so that the ECU can be optimized to increase the energy efficiency of a diesel engine powered by these biofuels, which can improve the results obtained by previous authors who studied their usage but without ECU recalibration. The engine tested in the present work is the one most commonly used in Brazil for land transport and, according to Brazilian regulations, must be tested following the ESC procedure. The engine performance and emissions test results obtained in this study are consistent with our understanding of their physicochemical properties and support the use of these biofuels in diesel engines. On top of all of this, it is important to highlight the potential positive contribution of these biofuels to the energy policy and the social economy in Brazil, which is certainly significant based on the impact of sugarcane bioethanol on the nation.

This study makes two addition novel contributions: Firstly, the use of the ratio of exhaust gas temperature (T_g) to available energy per cycle (*ec*) to analyze the variations observed in exhaust emissions, which can be considered an important contribution to the body of knowledge since it provides an estimation of the energy conversion into work per cycle (this energy is usually determined from the pressure curves in the combustion chamber). Secondly, the experimental verification of the inhibition process of CO at the DOC for alternative fuels with respect to diesel fuel, which supports the claim of previous authors.

2. Materials and methods

2.1. Tested fuels

Table 1 shows the properties of the three fuels tested. The reference fuel is S50, a blend of mineral diesel and 5% biodiesel available at fuel stations throughout Brazil. S50 is compared to sugarcane biodiesel and sugarcane diesel-farnesane.

Table 1. Properties of the tested fuels

Property	**Unit**	**Diesel S50**	**Sugarcane diesel-farnesane**	**Sugarcane biodiesel[a]**
Approximate summarized formula	[-]	$C_{15.2}H_{27.3}$[b]	$C_{15}H_{32}$	$C_{16}H_{30}O_2$
H/C		1.796	2.133	1.875
Cetane number	[-]	49.0	58.7[d]	69.9[c,d]
Density at 20 °C	kg L^{-1}	0.843	0.770	0.875
Viscosity at 40 °C	mm^2 s^{-1}	3.110	2.710	3.326
Lower heating value (LHV)	MJ kg^{-1}	42.03	43.43	35.80
Lower heating value	MJ L^{-1}	35.43	33.44	31.32
Stoichiometric air-fuel ratio $(A/F)_{st}$	[-]	14.50	14.98	12.23
$LHV/(A/F)_{st}$	MJ kg_{air}^{-1}	2.899	2.899	2.927
Distillation 10% vol	°C	196.0	250.5	280.0
Distillation 50% vol	°C	260.0	252.0	294.0
Distillation 90% vol	°C	340.0	254.0	306.0

[a]Conforming to the requirements and test methods for fatty acid methyl esters specified in the EN-14214

standard.

[b]the oxygen was not considered due to its low mass fraction.

[C]Out of measurement range (< 60).

[d]DCN (Derived Cetane Number). Measured by an alternative method based on infrared spectrometry according to the ASTM D6890 standard followed in Brazil.

2.2. Experimental test bench

A medium-sized diesel engine, fueled with the studied fuels, was run following Proconve P7, which is the Brazilian version of Euro V for controlling pollution from vehicles. Table 2 lists the main characteristics of the engine, which includes an Exhaust Gas Recirculation system (EGR).

Table 2. Engine specifications

Engine Model	**MAN D0834 LF05**
Operation	Diesel, four stroke
Supercharging	two-stage forced induction (2 turbochargers)
Intercooling	2 intercoolers
Cylinders	4 in line
Displacement	4.58 liters
Bore/Stroke	108 mm/125 mm
Compression ratio	16.5:1
Max power at 2400 min^{-1}	166 kW
Max Torque at 1100 - 1600 min^{-1}	850 Nm
Injection System	Electronic Common Rail
Emissions Standards	Euro V

The engine tests were performed on an experimental test-bench equipped with a motoring AVL APA 220 Dynamometer, which can measure up to 220 kW power, 930 N m torque and 10000 min^{-1} engine speed. The analysis of the exhaust gas collected before and after the Diesel Oxidation Catalyst (DOC) using an AVL AMA i60 gas analyzer provided the engine emissions. An AVL Smart Sampler was used to measure the particulate emissions (PM) under steady-state or

179 transient conditions. It is a dilution system of a partial flow of the engine exhaust with filtered
180 air, designed for the gravimetric sampling of exhaust particulates by collecting them in a filter.
181 Fig. 1 shows the experimental test bench used in this study, and Table 3 shows its main
182 specifications. The experimental set-up is the same as the one described in [9].

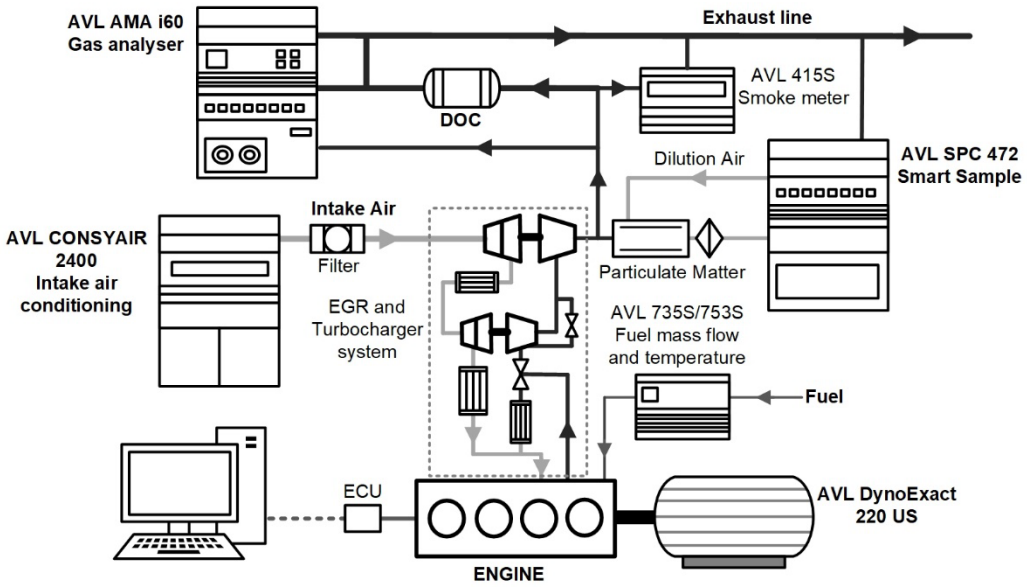

183

184 Fig. 1. The engine test bench. Icons qualitatively show the size and distribution of the engine components and
185 measurement devices.

186 Table 3. Specifications of the experimental devices.

Equipment	**Parameter**	**Range [units]**	**Accuracy**
AVL 735S / 753S	Fuel mass flow	0 ÷ 125 [kg/h]	±0.12%
	Fuel supply temperature	-10 ÷ 40 [ºC]	
ABB Sensy flow FMT700-P	Air flow ratio	1:40	±2 % air mass
AVL Intake air conditioning CONSYSAIR 2400	Temperature	-40 ÷ +60 [ºC]	± 0.5 [ºC]
	Pressure	-400 ÷ 200 [mbar]	± 1 [mbar]
	Moisture	4 ÷ 34 [g H_20/kg dry air]	
Vaisala HMT333	Intake air temperature	-40 ÷ +60 [ºC]	± 0.2 [ºC]
	Intake air humidity	0 ÷ 90% /90% ÷ 100%	± 2%/± 3%
AVL DynoExact 220 US (Active dynamometer)	Torque	0 ÷ 934 [Nm]	± 0.1%
	Speed	0 ÷ 10000 [rpm]	

		Power		0 ÷ 220 [kW]	
AVL Emissions test bench AMA i60	FID: Flame Ionization Detector	Emissions measurement:	Total hydrocarbon (THC) CH_4	THC: 10 ÷ 20000 [ppm] CH_4: 30 ÷ 20000 [ppm]	± 0.5%
	CLD: Chemilumines-cence Detector		NO, NO_X	3 ÷ 1000 [ppm]	± 0.5%
	IRD: Infrared Detector		CO, CO_2	CO: 50 ÷ 5000 [ppm] CO_2: 0.1 ÷ 6 Vol%	± 0.5%
	PMD: Paramagnetic Detector		O_2	0 ÷ 25%	± 0.5%
	LDD: Laser Diode Detector		NH_3	5 ÷ 1000 [ppm]	± 0.5%
	QCL: Quantum Cascade Laser		N_2O	5 ÷ 1000 [ppm]	± 0.5%
AVL 415S (filter paper blackening)		Soot concentration		1 ÷ 10 FSN [Filter Smoke Number]	±0.02 [mg/m³]
AVL Smart Sample SPC 472		-		-	-
Micro Balance XP2U		Particulate matter		0.00003 ÷ 2.1 [g]	±0.0001 [mg]

2.3. Description of the experimental tests

The Brazilian standard ABNT NBR 15634 [20] for road vehicles was applied for quantitatively determining the harmful emissions NOx, CO, HC, PM, and smoke. This standard is based on two types of testing cycles: a test cycle consisting of a sequence of steady-state modes defined by load and engine speed (the European Stationary Cycle – ESC), and transient cycles (the European Transient Cycle – ETC and the European Load Response – ELR engine test). Input boundary conditions were the same during the tests of each of the three fuels.

2.3.1. The ESC test cycle

196 The ESC test cycle explains how to measure pollutant gas emissions and PM emissions of an
197 engine working under a 13-mode steady-state procedure. NO_x, CO and THC emissions, as well
198 as the exhaust emissions flow and engine power are measured during each mode and averaged
199 over the cycle using a set of weighting factors. Particulate matter emissions are collected by
200 diluting the exhaust gas with conditioned air and sampled on one filter over the 13 modes. The
201 final emission results are expressed in g/(kW h).

202 The ESC test requires the definition of three engine speeds (*A*, *B* and *C*). The *A*, *B* and *C* speeds
203 to run the test depend on (i) the high speed n_{hi} determined by calculating 70% of the declared
204 maximum net power, (ii) the low speed n_{lo} determined by calculating 50% of the declared
205 maximum net power and (iii) the following equations:

206 $$A = n_{lo} + 0.25(n_{hi} - n_{lo}), \quad (1)$$

207 $$B = n_{lo} + 0.50(n_{hi} - n_{lo}), \quad (2)$$

208 $$C = n_{lo} + 0.75(n_{hi} - n_{lo}). \quad (3)$$

209 The estimation of n_{hi} and n_{lo} requires the full load engine curves for the three fuels defined
210 according to ABNT NBR 1585 standard [21] (see Fig. 2).

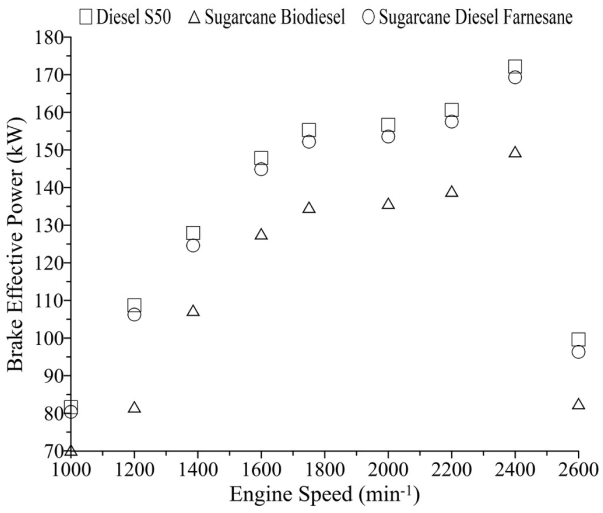

211

212 Fig. 2. Power curves at full load.

213 According to Fig. 2, the brake effective power changes for each tested fuel due to their
214 different LHV, such as observed in a previous study [9]. Consequently, the engine speeds *A*, *B*,

215 and *C* differ for each fuel (see Table 4) since their calculation depends on the maximum power
216 (see Eq. (1) to (3)). Fig. 3 shows the ESC modes tested in the present work.

217 Table 4. Modes calculated according to the specifications of the ESC test [21], for the engine and fuels tested.

Point	Mode	Engine speed (min^{-1})				Torque (%)	Weight factor W_F	Duration (min)
		Symbol	Mineral diesel S50	Sugarcane Biodiesel	Sugarcane diesel-farnesane			
1	1	idle	700	700	700	0	0.15	4
2	7	A	1398	1559	1410	25	0.05	2
3	5	A	1398	1559	1410	50	0.05	2
4	6	A	1398	1559	1410	75	0.05	2
5	2	A	1398	1559	1410	100	0.08	2
6	9	B	1762	1884	1787	25	0.10	2
7	3	B	1762	1884	1787	50	0.10	2
8	4	B	1762	1884	1787	75	0.10	2
9	8	B	1762	1884	1787	100	0.09	2
10	11	C	2127	2209	2163	25	0.05	2
11	13	C	2127	2209	2163	50	0.05	2
12	12	C	2127	2209	2163	75	0.05	2
13	10	C	2127	2209	2163	100	0.08	2

218 Note: the testing sequence follows the numerical order of the modes, which entails the following
219 order of points: 1, 5, 7, 8, 3, 4, 2, 9, 6, 13, 10, 12, and 11. Graphics were built based on the sequence
220 of points.

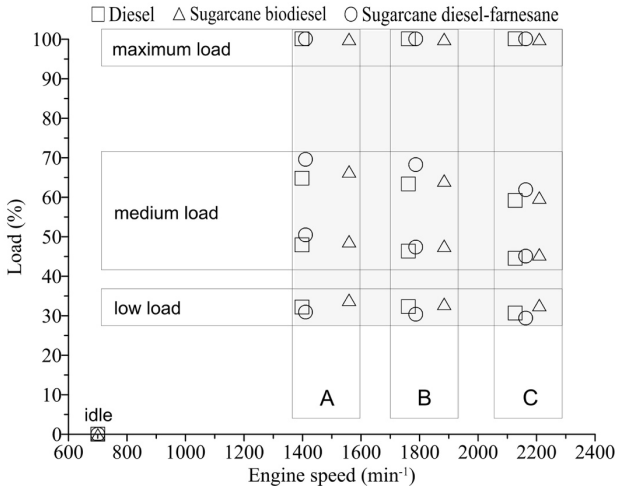

Fig. 3. Modes of the ESC test cycle

The engine was operated for 2 minutes in each mode, except for the idle mode that lasted 4 minutes (Table 4). Approximately 20 seconds were used to stabilize the engine speed and torque in each mode. The specified speed was held to within ±50 rpm, and the specified torque was held to within ±2% of the maximum torque at the test speed.

Pollutant concentrations were measured on a dry basis. Nevertheless, since the pollutant of the exhaust gases was actually on a wet basis, the conversion to a wet basis was done following the specifications of the standard ABNT NBR 15634 [20]. In addition, since NOx emissions measurements depend on the ambient air temperature and humidity conditions, their concentrations were corrected through the correction factor ($k_{h,d}$) provided by the aforementioned standard.

Mass flow emissions (m_{gas}) in g/h for each mode and for each gaseous component were calculated by Eq. (4) and (5):

$$m_{gas} = u_{gas}\, C_{gas}\, q_{mew}, \quad (4)$$

$$m_{gas} = u_{gas}\, C_{gas}\, q_{mew}\, k_{hd} \text{ (for NOx)}, \quad (5)$$

where u_{gas} is the relationship between the density of a determined pollutant and the density of the exhaust gases. The reference [17] provides the following u_{gas} values assuming ideal gas properties: u_{NOx} = 0.001587, u_{co} = 0.000966, u_{THC} = 0.000479, and an exhaust gas density 1.293 kg/m^3 (air density at 273 K and 101.3 kPa). C_{gas} is the concentration of the exhaust gas

component, measured in the exhaust gas, in ppm, and q_{mew} is the mass flow of the exhaust gases (kg/h).

Finally, the specific emissions in g/(kW h) were determined for each exhaust gas component (gas_x, x=NOx, CO, THC) as the average of the emissions in each mode ($m_{gas\ i}$, i=1, 2,…,m=13) weighted by the set of factors (W_{Fi}) listed in Table 4:

$$gas_x = \frac{\sum_{i=1}^{m}(m_{\mathrm{gas}\ i}\, W_{\mathrm{F}\ i})}{\sum_{i=1}^{m}(P_{\mathrm{f}\ i} W_{\mathrm{F}\ i})}, \quad (6)$$

where P_f, f= (S50, Diesel-farnesane, Sugarcane-biodiesel) is the engine power in kW.

PM emissions mass flow (PT_{mass}) in g/h was calculated through the measured particulate matter over the 13 modes (m_f) and the value of the average mass flow of exhaust gas diluted with moist air (q_{medf}) weighted for each mode according to the weight factor (W_{Fi}) presented in Table 4. To measure the mass of particles, special filters were used together with a high precision scale to determine the weight of the filter before and after each test. Specific PM emissions were calculated by Eq. (7):

$$PM = \frac{PT_{\mathrm{mass}}}{\sum_{i=1}^{m}(P_{\mathrm{f}\ i} W_{\mathrm{F}\ i})}. \quad (7)$$

The standard limits for particulate matter and specific pollutant emissions on the ESC test are: PM (0.02 g/kW h), CO (1.5 g/kW h), HC (0.46 g/kW h), NOx (2.0 g/kW h) [22].

2.3.2. Experimental results under the same values of performance

As previously explained, the ESC test was performed to determine if the specific emissions of exhaust gases and particulates meet the standard limits. In addition to the comparative study of the specific emissions for the three fuels tested, the results obtained were used for analyzing the performance and emissions (g/h) for each of these 13 steady-state modes. Figure 4 shows that each fuel produces different values of engine torque and speed during the ESC test. Hence, in the present section, the analysis of the effect of the properties of each fuel on engine emissions is performed for the same effective power delivered by the engine. This analysis is recommended by previous authors [23], who suggest maintaining the same speed and torque

266 for a meaningful comparison. Table 5 shows the characteristic values of the selected operating
267 regimes that provide the same power for the three fuels tested.

268 Table 5. Characteristics values of the steady-state operating modes selected.

Mode	*n* Engine speed (min^{-1})	*T* Engine Torque (N m)	Power $P = \frac{n\,T}{9549.3}$ (kW)	P_e Mean effective pressure (MPa)	Load (%)
Z_1	1600	300	50.27	0.82	34
Z_2	1600	500	83.78	1.37	56
Z_3	1600	700	117.29	1.92	79
Z_4	1750	250	45.81	0.69	29
Z_5	1750	450	82.47	1.23	52
Z_6	1750	650	119.12	1.78	75
Z_7	1950	210	42.88	0.58	26
Z_8	1950	450	91.89	1.23	56
Z_9	1950	650	132.73	1.78	81
Z_{10}	2100	200	43.98	0.55	27
Z_{11}	2100	400	87.96	1.10	54
Z_{12}	2100	600	131.95	1.65	81

269 Fig. 4 shows the Z_i modes (i= 1, 2, 3…12) that represent the same engine power provided by the
270 three fuels tested, as well as the 12 modes of the ESC test cycle (without the idle condition).

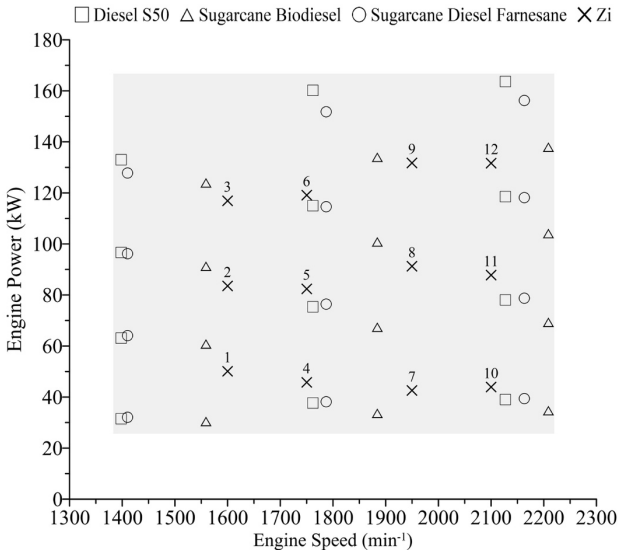

Fig. 4. Z_i modes where the three fuels provide the same engine power and 12 ESC modes without the idle condition.

The 12 modes Z_i were selected as follows: first, the following four values of engine speed were set: 1600, 1750, 1950 and 2100 min^{-1}, and secondly, three different loads: low load (between 43 and 50 kW), medium load (between 82 and 92 kW) and high load (between 117 and 133 kW), were determined. These power ranges represent approximately 25, 50 and 75% of the nominal engine power. The values of the mean effective pressure P_e for each load were: P_e = 0.55-0.82 MPa for low load (26-34%, respectively); P_e= 1.10-1.37 MPa for medium load (52-56%, respectively); and P_e = 1.65-1.92 MPa for high load (75-81%, respectively).

2.3.3. Statistical analysis of the results

Each experimental response was obtained as the mean value of three tests: x_1, x_2, and x_3. The standard deviation *s* was calculated, as some engineering statistics texts suggest [24], using the range estimate for smaller sample sizes: $s = x_{max}\text{-}x_{min}/d(k)$; in our case $d(k=3) = 1.693$. The uncertainty of the result of each measurement was obtained by applying a coverage factor of 2, which led to a coverage probability of 95%, except for the case of the PM emissions (70% coverage probability). The uncertainty of the results obtained via equations was calculated applying the law of propagation of uncertainty according to the "Guide to the expression of uncertainty in measurement" [25]. Spurious data were removed according to the Chauvenet's criterion.

3. Results

3.1. Engine performance under the ESC test

The brake specific fuel consumption (*bsfc*) and the thermal efficiency of the engine (η_t) for the 3 fuels are shown in Figs. 5a and 5b respectively. The low engine power in points 2, 6, and 10 (A_25%, B_25%, and C_25%) (see Fig. 6a) led to a higher *bsfc* compared to the medium and maximum load modes. Comparing the fuels, the *bsfc* of sugarcane biodiesel was the highest and that of sugarcane diesel farnesane was the lowest, which is in agreement with their LHV (see Table 1). Fig. 5b shows that sugarcane biodiesel provides higher brake thermal efficiency at full load than diesel S50, documented in points 5, 9, and 13 (A_100%, B_100%, and C_100%). At 75% load, η_t is nearly the same (points 4, 8, and 12 corresponding to A_75%, B_75%, and C_75%) for these two fuels, and at 50% and low load, sugarcane biodiesel has the lowest thermal efficiency (points 3, 7, and 11 corresponding to A_50%, B_50%, and C_50% and points 2, 6, and 10 corresponding to A_25%, B_25%, and C_25%, respectively). The significantly higher *bsfc* of sugarcane biodiesel at low load (points 2, 6, and 10 in Fig. 5a) is responsible for the low thermal efficiency of sugarcane biodiesel at these operating regimes. Summarizing, the combustion efficiency improves for all tested fuels as the load increases. Nevertheless, the sugarcane biodiesel shows a greater improvement compared to the reference fuel S50. On the other hand, sugarcane diesel-farnesane shows the greatest thermal efficiency for all operating regimes.

According to Table 1, LHV varies for each fuel, but is noted in Fig. 5 that the differences in *bsfc* among the tested fuels are considerably more significant than the differences among their efficiencies. Hence, assuming that thermal efficiency is constant, and considering that η_t = 3600/(*bsfc*·LHV), it can be concluded that the LHV is responsible for the observed differences in *bsfc*. It is interesting to note that, although the LHV varies for each fuel tested, the value of the ratio $LHV/(A/F)_{st}$ is nearly the same (see Table 1), which agrees with the statement made by previous authors [26] who claimed that, for liquid fuels employed in vehicles engines, this ratio changes within narrow limits and may be assumed to be constant $LHV/(A/F)_{st}$= 3.0 MJ kg_{air}^{-1}.

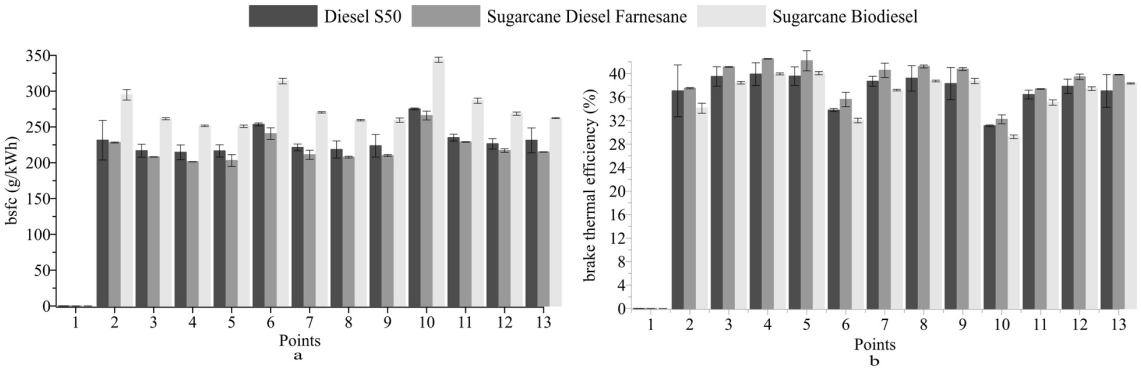

Fig. 5. a) Brake specific fuel consumption and b) Brake thermal efficiency (η_t).

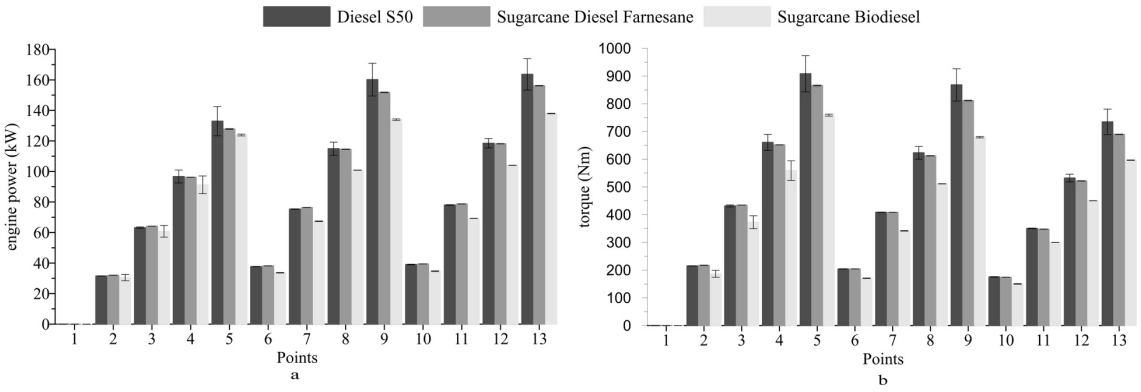

Fig. 6. a) Engine power, b) torque.

It is also interesting to analyze the air consumption required to burn the injected fuel. The fuel-air equivalence ratio ϕ is the ratio of the actual fuel-air ratio F/A to the stoichiometric fuel-air ratio $(F/A)_{st}$ [27], which is the inverse of the parameter $(A/F)_{st}$ listed in Table 1. According to Fig. 7a, the coefficient ϕ is quite similar for the three fuels in each test mode. This uniformity is even higher than that observed on efficiency (Fig. 5b). Therefore, the coefficient $\chi = \eta_t \cdot \phi$ varies in a narrow range for the three fuels in each operating condition (see Fig. 7b).

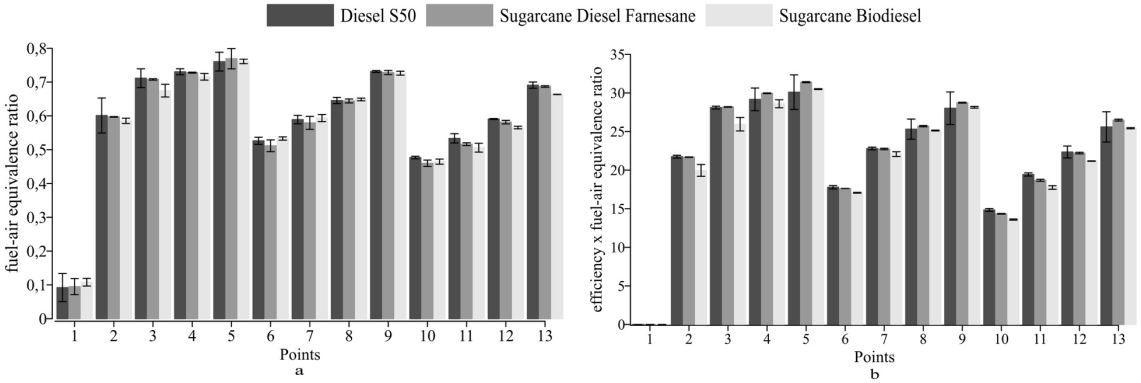

Fig. 7. a) Fuel-air equivalence ratio (ϕ), b) product of thermal efficiency and fuel-air equivalence ratio (χ).

Fig. 8a shows the exhaust gas recirculation mass flow (m_{EGR}), which was calculated through a simplified enthalpy balance considering the intake air and the recirculated exhaust gas [28]. In most test modes, the oxygenated fuel (sugarcane biodiesel) shows the largest amount of exhaust gas recirculation mass flow. The ECU manages the EGR so that the amount of oxygen in the exhaust gases is approximately the same for the three fuels tested (see Fig. 8b). Consequently, for the case of sugarcane biodiesel, which is the fuel with the lowest energy content, the ECU increases the fuel consumption (Fig. 9a) and, especially for tests at higher speeds (B and C), decreases air consumption (Fig. 9b).

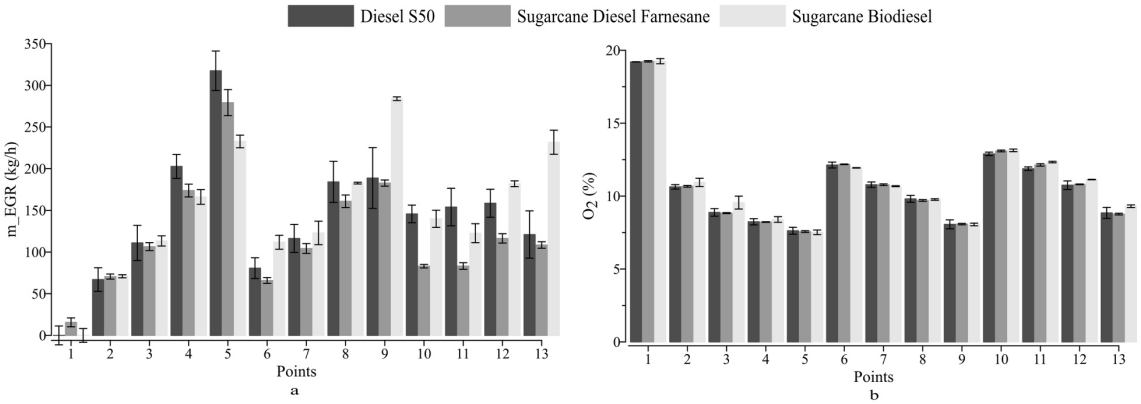

Fig. 8. a) Exhaust gas recirculation mass flow, b) the percentage of oxygen in the exhaust gases.

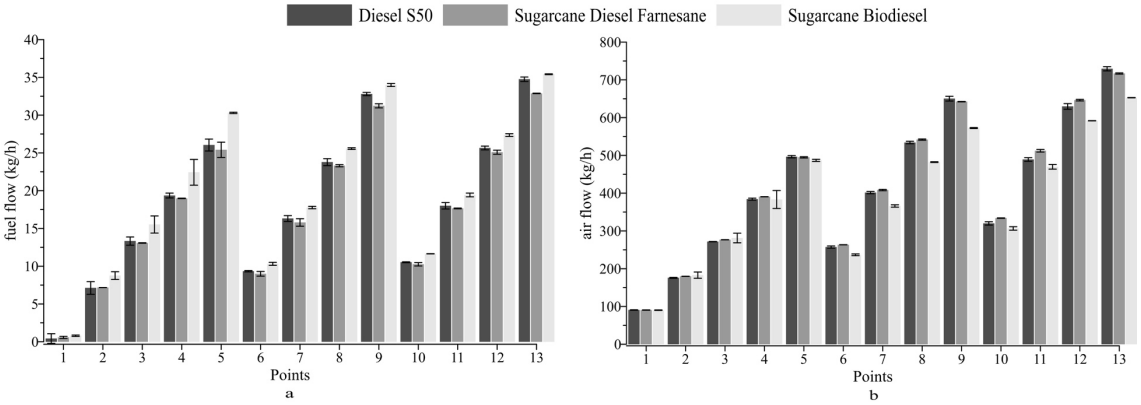

Fig. 9. a) Engine fuel consumption, b) intake air mass flow rate.

Fig. 10 shows the mass of fuel supplied per cycle (fueling). The largest fueling, which corresponds to the maximum torque in diesel engines (point 5 of Fig. 6b), is limited so that it provides a maximum value of χ or a minimum particle formation (PM). It is believed that this operating condition is close to the smoke limit despite having the largest gas recirculation.

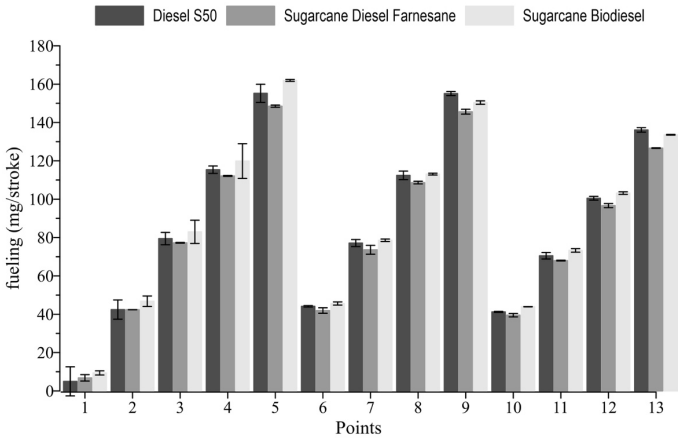

Fig. 10. Mass of fuel supplied per cycle (fueling).

These results indicate that a way to improve the power and torque performance (Fig. 6) of an engine running with sugarcane biofuels is by modifying the ECU map (which is usually optimized for mineral diesel fuel). It follows that engine emissions must be analyzed before optimizing engine performance.

3.2. Engine emissions

According to the current regulations in Brazil on emissions for on-road medium and heavy-duty vehicles, the controlled compounds are CO, THC, NO_x, and PM. The variation in exhaust gas emissions and PM, when using different fuels, can be obtained in different ways. In this work, specific emissions are obtained from the ESC test and compared with the limits established by the regulation (see the end of Section 2.3.1).

Based on the experimental results of specific emissions, the impact of the fuel chemical composition and its properties on gas emissions (NO_x, CO, and THC) in g/h for each test mode of the ESC test cycle is investigated. This analysis is also performed considering a set of Z_i steady-state modes; in each Z_i mode, the three fuels provided the same engine power, which helps to compare and analyze the differences in emissions among the tested fuels. The PM emissions analysis (in g/h) is carried out for the entire ESC test, i.e., the results show the PM emission accumulated over the 13 test modes.

3.2.1. Particulate matter

Fig. 11a shows the specific PM emissions obtained from the ESC test were computed by Eq. (7) for the three fuels tested. They are all below the limit established by the regulation (0.02 g/kW h). Specific emissions vary not only due to the variation in engine power (denominator of Eq. (7): $\sum_{i=1}^{m}(P_{\mathrm{f}i}\, W_{\mathrm{F}\,i})$, where P_f= 82.28 kW, 72.72 kW, 80.73 kW for diesel S50, sugarcane biodiesel, and sugarcane diesel farnesane respectively), but also due to the variation in PM emissions mass flow in g/h (numerator of Eq. (7): PT_{mass}) as shown in Fig. 11b. Compared to the reference diesel fuel, PM emissions in g/h decreased by 32.4% for sugarcane biodiesel and 41.7% for sugarcane diesel-farnesane.

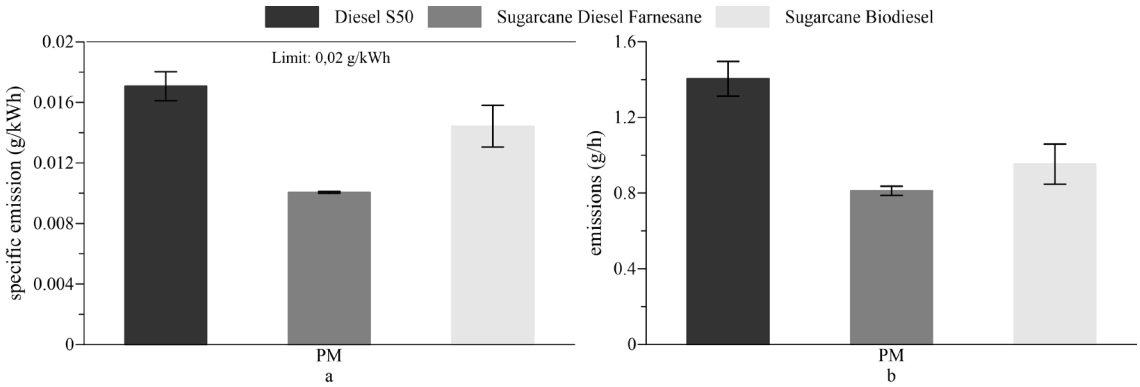

Fig. 11. a) Specific PM emissions, b) PM emissions mass flow (g/h) (PT_{mass}).

The diffusive combustion, characteristic of diesel engines due to the formation of heterogeneous fuel-air mixtures, causes considerable soot formation. The reason is the super-enriched areas where the molecular decomposition of the fuel takes place without enough air supply, which results in solid carbon emission. The chemical properties of fuels greatly influence diffusive combustion because the amount of evaporated fuel and the burning rate depend on them. The results show that these properties are favor sugarcane diesel-farnesane. This work corroborates the low specific PM emission of this biofuel observed by previous authors [9, 18]. Fig. 11b shows that sugarcane diesel-farnesane produces lower PM emissions than those of the diesel S50, which is explained by a shorter combustion stage, due to a higher cetane number. A previous study on sugarcane diesel-farnesane [5] showed little or no tendency to produce soot precursors. These precursors are short-chain dehydrogenated hydrocarbons, typically C_2H_2, that

385 combine to form polycyclic aromatic hydrocarbons. Many of these aromatic rings form soot
386 particles [29].

387 The lower PM emission of sugarcane biodiesel compared to those of diesel S50 is explained
388 by the absence of aromatic compounds, which reduces particle formation [30, 31], and by the
389 presence of oxygen in its chemical composition [28, 32]. The oxygen promotes soot oxidation in
390 the flame front and partial oxidation of the rest of the soot during the expansion process.
391 Although there is not a flame front in diesel engines during the combustion process, the results
392 obtained seem to point out that something very similar is happening. Part of the soot initially
393 formed in super-enriched areas oxidizes during the turbulent diffusion process, which takes
394 place in the expansion stroke thanks to the excess of O_2. This excess of O_2 is also observed in the
395 fuel-air equivalence ratio (ϕ) (Fig. 7a), which is slightly lower for the sugarcane biodiesel, despite
396 the higher gas recirculation in most modes (Fig. 8a).

397 Since sugarcane biodiesel is an oxygenated fuel, the amount of recirculated exhaust gas is
398 higher. This fuel promotes a NO_x emission reduction without compromising PM emissions. Even
399 more, previous authors found out that biodiesel soot is highly reactive to oxygen [33]. According
400 to reference [34], the smaller mean particle diameter of biodiesel contributes to increasing
401 oxidation reactivity of the soot, which promotes soot oxidation in the last stages of the
402 combustion process, as well as in the exhaust before dilution and measuring.

403 It is worth noting that the PM oxidation is a challenging phenomenon to understand due to
404 the complex stages involved in this process, and the short time in which they occur. A model of
405 the dynamics of soot particles was addressed in a previous work [35]. This new approach
406 provides a detailed physicochemical view of the formation and PM oxidation processes inside
407 the combustion chamber of the engine. The results of this study appear to support the claim
408 that oxygenated fuels promote the oxidation of PM.

409 The physicochemical properties of sugarcane biodiesel also explain the reduction of PM
410 compared to the reference diesel fuel. The ECU increases the fuel consumption for sugarcane

411 biodiesel (Fig. 9a) because it is the least energetic fuel achieved by means of a greater advance
412 of the injection timing and a longer injection duration [36]. This fact can explain the reduction
413 of PM emission [34].

414 The benefits of using oxygenated fuels for soot reduction are reported in many publications.
415 The presence of oxygen and the lack of aromatics in the fuel are presented as the main causes
416 of this reduction. The lower PM emissions of sugarcane diesel-farnesane are explained by the
417 higher hydrogen content and the absence of aromatics compounds [37-43] (see the values of
418 the H/C ratio in Table 1).

419 It is worth mentioning that, for all the fuels tested, mode 5 was the one that produced the
420 highest PM emission. This mode corresponds to the maximum torque and, consequently, to the
421 highest fuel supply per cycle, which is limited in such a way that it provides a maximum value of
422 χ for a minimum PM formation. It is believed that this operating condition is close to the smoke
423 limit, despite having the largest gas recirculation.

424 **3.2.2 Exhaust gas emissions**

425 *NO_x emissions*

426 Fig. 12 shows the NOx emissions after DOC for the ESC test cycle. Eq. (5) and Eq. (6) were
427 used to determine the NOx mass flow (Fig. 12b) and specific NOx emissions (Fig. 12a),
428 respectively. Both sugarcane biodiesel and sugarcane diesel-farnesane show NOx values below
429 the regulation limit (2.00 g/kW h). Compared to the reference diesel fuel, NOx emissions in g/h
430 decreased by 37.3% for sugarcane biodiesel and 6.98% for sugarcane diesel-farnesane. Specific
431 NOx emissions of diesel S50 (2.20 g/kW h) are above the standard limit, most likely because the
432 ECU was not recalibrated for this fuel.

433 Fig. 13 shows the NOx mass flow in each mode of the ESC test cycle. NO_x emissions of
434 sugarcane biodiesel are lower than those of the S50 in all modes, except for modes 11 and 13
435 (points 10 and 11), which correspond to 25% and 50% load respectively.

Engine performance is different for the three fuels in each mode (Fig. 6a) therefore, it seems appropriate to analyze the emissions of the three fuels under the same values of effective power. Fig. 14 shows NO_x emissions for the Z_i modes listed in Table 5. Fig. 13 and Fig. 14 show similar results.

The lower NO_x emissions of biofuels are due to the lower flame temperatures and oxygen concentrations produced by the EGR [44]. The higher cetane number and H/C ratio produce lower flame temperatures [15,45]. This can be verified by observing the exhaust gas temperatures (Fig. 15), measured at the exhaust manifold, just before the input of the turbine 2 (see Fig. 1). Lower exhaust gas temperatures indicate lower maximum combustion temperatures. Note that for all ESC conditions (Fig. 15a), sugarcane diesel-farnesane shows the lowest exhaust gas temperature, and the reference fuel S50 the highest one. It is clear from Fig. 15b that the exhaust gas temperatures are similar for all fuels at all operation modes Z_i (with the same engine power for the three fuels).

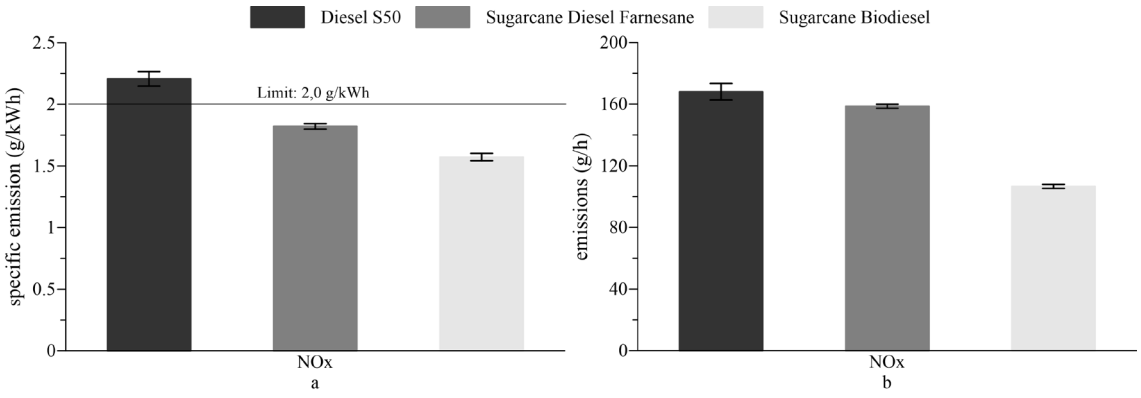

Fig. 12. NOx emissions of the ESC test cycle after DOC: a) specific emissions, b) mass flow emissions (g/h).

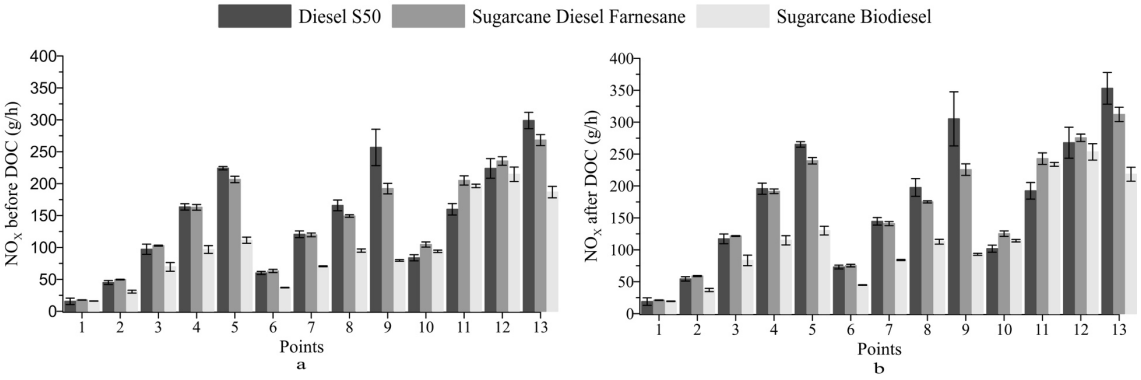

Fig. 13. NOx mass flow emissions g/h at each ESC mode: a) before DOC and b) after DOC.

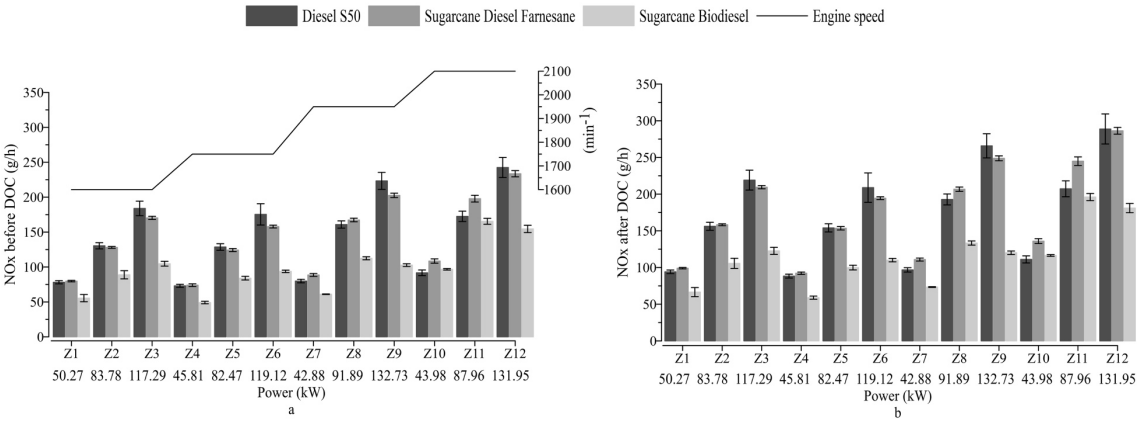

Fig. 14. NOx mass flow emissions (g/h) and engine speed (min^{-1}) for the three fuels in each Z_i mode: a) before DOC and b) after DOC.

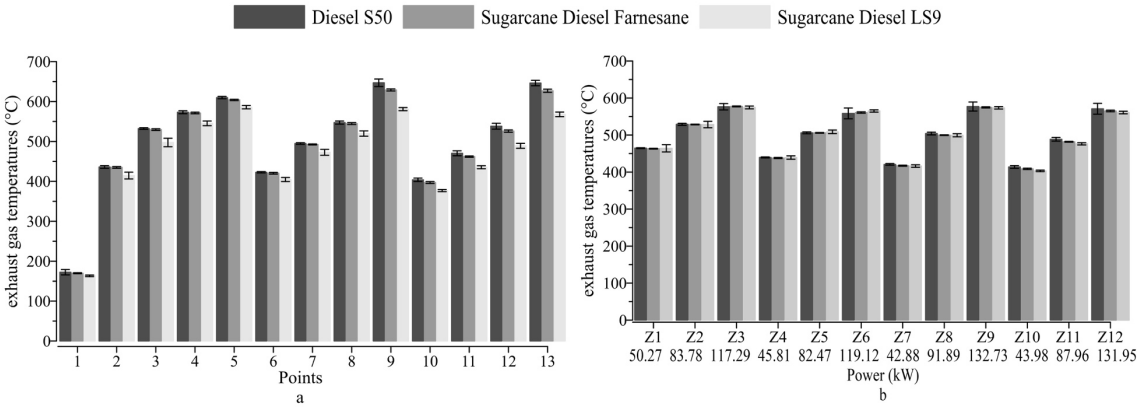

Fig. 15. Temperature of the Exhaust gases: a) 13 modes of the ESC test, b) Z_i modes (the same effective power provided by the three fuels).

Since it was not possible to measure the pressure in the combustion chamber, the indicated work was not determined. Nevertheless, the amount of input energy per cycle (available energy per cycle "*ec*") can be calculated according to Eq. (8). Fig. 16b shows the *ec* results obtained for each fuel.

$$ec = \text{fueling} \cdot 10^{-3} \cdot LHV. \quad (8)$$

According to Fig. 16b, biofuels show similar or greater *ec* values than S50 for most Z_i modes.

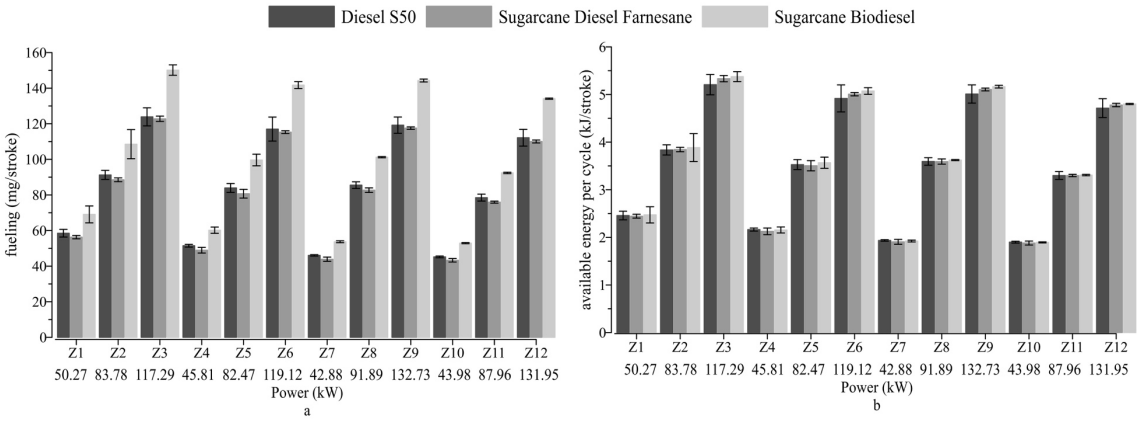

Fig. 16. Z_i modes (each mode provides the same engine power): a) fueling b) available energy per cycle (*ec*).

The ratio of exhaust gas temperature T_g to *ec* provides the increase of temperature per kJ of available energy in a cycle (Fig. 17). Low values of that ratio are related to low flame temperatures and, therefore, to low NOx emissions. Except for the Z4, Z5, and Z7 modes, biofuels have lower T_g/*ec* values than S50, especially sugarcane biodiesel, which has the greatest exhaust gas recirculation mass flow (Fig. 18) and, hence, the lowest NOx emissions.

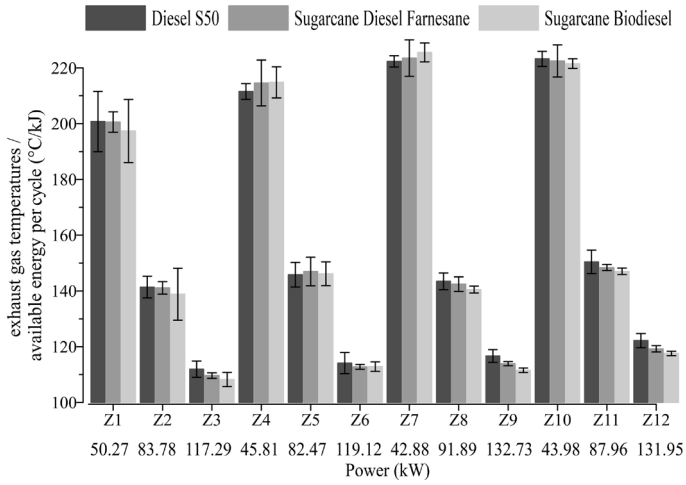

Fig. 17. Ratio of exhaust gas temperature to available energy per cycle for the three fuels at each Z_i mode.

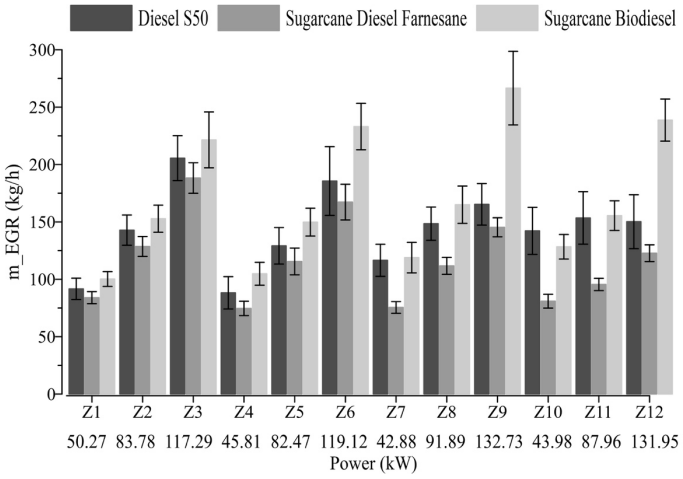

Fig. 18. Exhaust gas recirculation mass flow (*m*_EGR) for the three fuels at each Z_i mode.

Although the engine running with sugarcane diesel-farnesane has the lowest exhaust gas recirculation mass flow (Fig. 18), this fuel has, in general, lower T_g/ec values than S50 and, therefore, lower NOx emissions. The reason can be found in its higher cetane number and H/C ratio that produce lower flame temperatures than S50 [15, 45]. An important contribution to the new body of knowledge on emissions analysis is the discovery of this relationship between the exhaust gas temperature and the available energy per cycle, which provides an estimation of the energy transformed into work per cycle. This energy is traditionally determined from the pressure curves measured inside the combustion chamber. It is worth discussing the small NO_x emissions increase noted after DOC (see Figs 13 and 14). DOC is intended for CO and THC reduction, and in the authors' opinion, two reasons can explain the observed NO_x increase:

i. NO_2 dissociation. The EGR technique reduces the flame temperature to reduce NO formation but increases N_2O formation [45]. N_2O can dissociate into NO by two mechanisms: blending with oxygen ($N_2O + O \Leftrightarrow NO + NO$) or hydrogen ($N_2O + H \Leftrightarrow NO + NH$).

ii. After DOC, the measurement error is greater than before DOC. The ratio NO_2/NO after DOC could be greater than before DOC due to a higher conversion of NO into NO_2. Considering that it is more difficult to get accurate measurements of N_2O than NO [45], the increase in NO_x emissions could be a result of the measurement error.

494 *CO emissions*

495 For all fuels tested, the specific CO emissions after DOC are well below the limit specified by
496 the regulation (1.5 g/kW h) (Fig. 19a). Diesel-farnesane and diesel-S50 emit a similar amount of
497 CO. On the other hand, sugarcane biodiesel produces much more CO than S50 and farnesane.
498 The lower engine power (denominator of Eq. 6) and the higher total CO emissions in g/h (Eq. 4
499 and Fig. 19b) explain the previous result. Compared to the reference diesel fuel, CO emissions
500 increased from 3.44 g/h to 7.29 g/h for sugarcane biodiesel and from 3.44 g/h to 3.57 g/h for
501 sugarcane diesel-farnesane.

502 In most operating regimes, the sugarcane biodiesel causes significantly lower CO emissions
503 before DOC than those of the rest of the fuels tested, however, those emissions after DOC are
504 always higher for all points of the ESC test (Fig. 20). Extending the idea of Majumdar, Pihl, and
505 Toops [46] to real fuels used in diesel engines, the chemical composition of sugarcane biodiesel
506 could inhibit the reduction process of CO at DOC, which would be consistent with the
507 experimental results obtained in the present paper.

508 Because the three fuels produce different engine powers at each point of the ESC test (Fig.
509 6a), it is also appropriate to analyze CO emissions at those Z_i modes listed in Table 5 in which
510 the three fuels provide the same engine power (see Fig. 21).

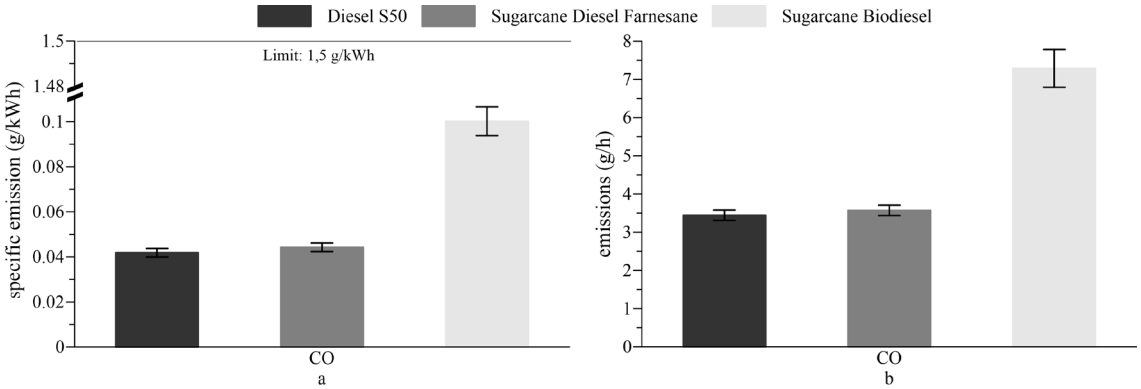

511

512 Fig. 19. Total CO emissions for the ESC test after DOC a) specific emissions, b) emissions in g/h.

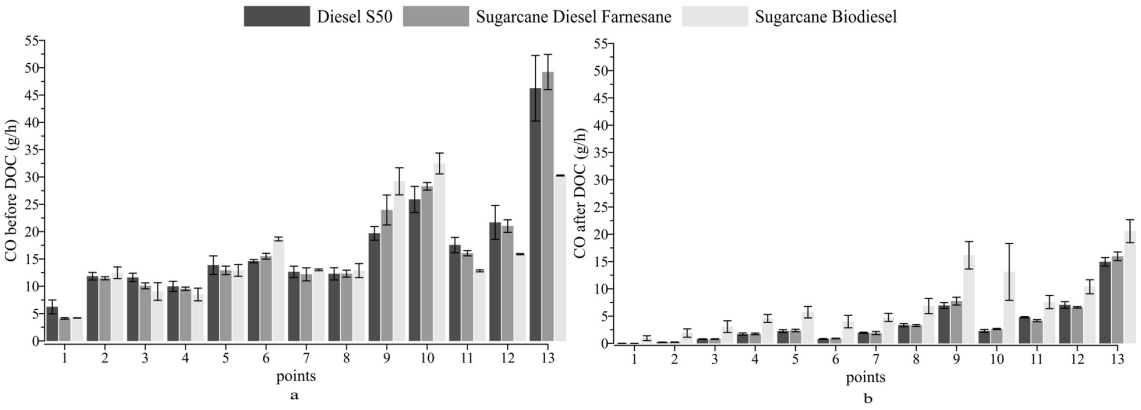

Fig. 20. CO emissions at each mode of the ESC test a) before DOC and b) after DOC.

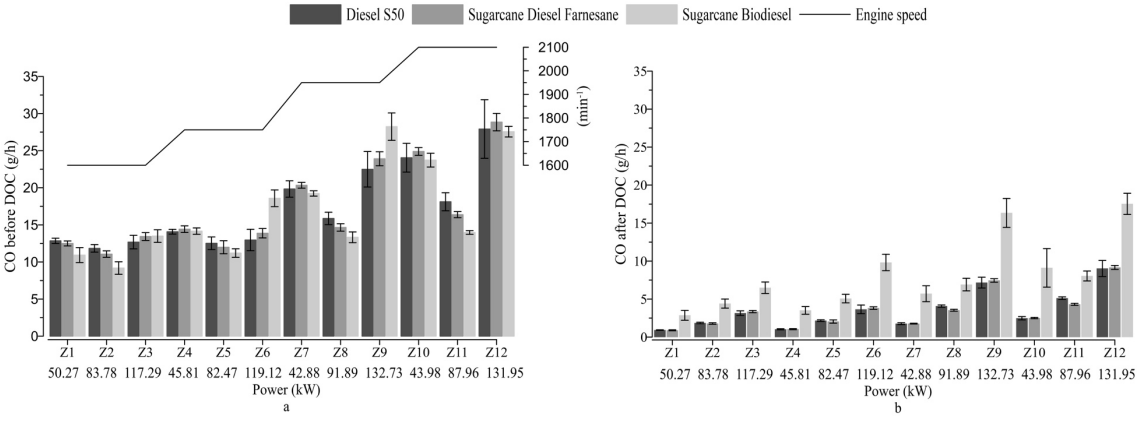

Fig. 21. CO emissions (g/h) and engine speed (min^{-1}) for the three fuels at each Z_i mode (each mode provides the same engine power): a) before DOC and b) after DOC.

According to Fig. 21a, CO emissions across all the fuels are minimized for the Z_i operating regimes at medium load and several engine speeds, i.e., Z_2, Z_5, Z_8, and Z_{11}, which means that combustion efficiency is enhanced at medium load. This fact can be observed in Fig. 21a, since Z_i modes to the right of the medium load modes (higher load for the same engine speed), as well as those to the left of these modes (lower load for the same engine speed), show higher CO emissions for the three fuels tested. Regarding these medium load regimens, biofuels produce lower CO emissions than diesel S50 and, in particular, sugarcane diesel-farnesane produce the lowest CO emissions.

Previous works on hydroprocessed biofuels showed that the increase in the cetane number (CN) decreases the ignition delay at low to moderate temperatures (650-900 K) [13, 14]. Hence, combustion is enhanced, and CO emissions decrease. This fact explains the results regarding CO

emissions at most Z_i modes, except for those modes at maximum loads (Z_3, Z_6, Z_9, and Z_{12}) where the vaporization process had more influence than the CN. Gowdagiri et al. [15] worked with the same fuels studied by [13, 14] and noted a moderate reduction in the ignition delay for significant changes in CN, which means that most of the ignition delay is due to the rate of vaporization rather than a chemical process. According to Table 1, the distillation characteristics of the biofuels (pure compounds) differ significantly from those of the reference diesel (mix of hydrocarbons), which can explain their higher CO emissions at maximum loads (Fig. 21a).

THC emissions

Fig. 22a shows the specific THC emissions after DOC. For all fuels tested, these emissions are well below the limit established by the regulation (0.46 g/kW h). Sugarcane diesel-farnesane produces the highest values since it shows the greatest THC emissions in g/h (Fig. 22b), which is a result of the highest THC emissions after DOC at each ESC mode (Fig. 23b). Compared to the reference diesel fuel, THC emissions in g/h increased from 0.58 g/h to 0.89 g/h for sugarcane diesel-farnesane but were reduced from 0.58 g/h to 0.49 g/h for sugarcane biodiesel. The low THC emissions of sugarcane biodiesel at all ESC modes before DOC (Fig. 23a) is noteworthy.

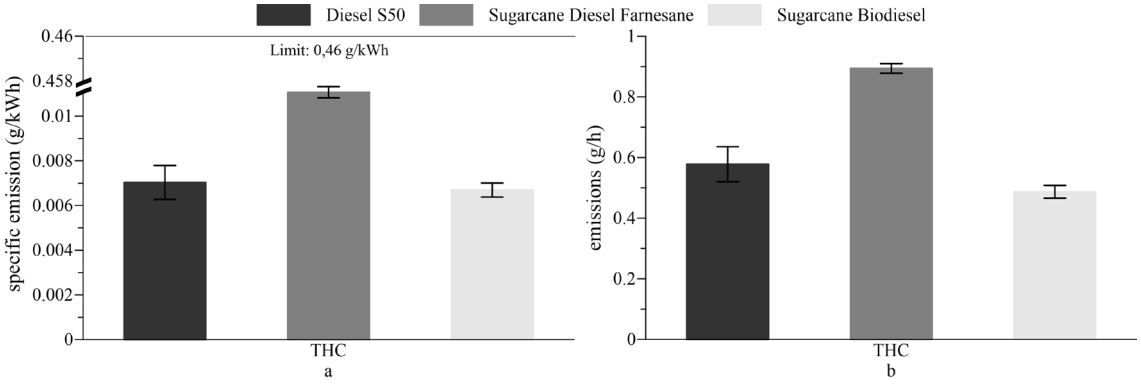

Fig. 22. THC emissions for the ESC test after DOC: a) specific emissions, b) THC emissions (g/h).

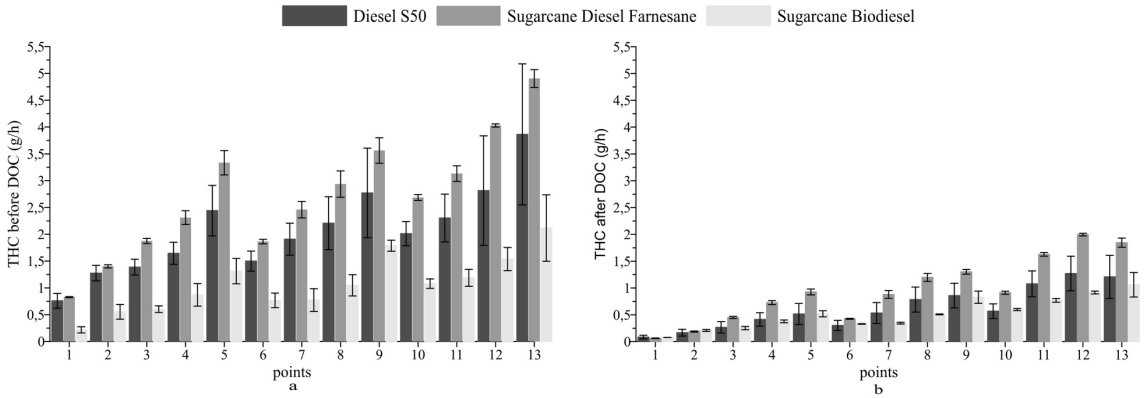

Fig. 23. THC emissions in g/h at each mode of the ESC test a) before DOC and b) after DOC.

As previously done for CO and NOx emissions, THC emissions were measured for the set of Z_i modes listed in Table 5. Again, in each Z_i mode, all tested fuels produce the same engine power. As shown in Fig. 24, the lowest THC emissions are for sugarcane biodiesel for all Z_i modes, while sugarcane diesel-farnesane produces the highest emissions. The higher THC emissions of sugarcane diesel-farnesane compared to diesel S50 can be explained by their different evaporation rate at different temperatures [15]. According to Table 1, sugarcane diesel-farnesane has a fairly homogeneous evaporation process. On the other hand, diesel S50, which is a mixture of hydrocarbons, has a considerable amount of evaporated mass at low temperature, which promotes the oxidation of the fuel at the initial stages of the combustion and, therefore, a reduction in THC emission.

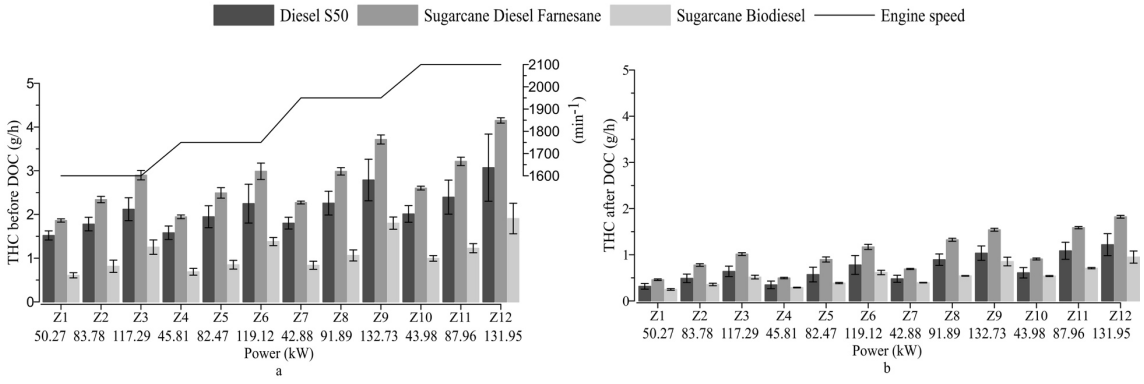

Fig. 24. THC emissions (g/h) and engine speed (min^{-1}) for the three fuels at each Z_i mode (each mode provides the same engine power): a) before DOC and b) after DOC.

A lower THC formation decreases the probability of formation and growth of PM by hydrocarbon condensation and adsorption on the particle surfaces [37]. In other words, if there

563 is less THC measured in the exhaust gases, it may be because a considerable part was absorbed
564 by the soot particles. Therefore, the relative increase of THC emissions observed for sugarcane
565 diesel-farnesane may be related to the reduction of its PM emissions, since the reduction in the
566 concentration of carbonaceous particles in the exhaust gas provides a smaller area available for
567 the absorption and condensation of hydrocarbons on the surfaces of these particles. Similar
568 behavior was observed in previous works [34, 47].

569 Sugarcane biodiesel produces the lowest THC emissions, both before and after the DOC (Fig.
570 24). The main factors contributing to this decrease in comparison to diesel S50 are the presence
571 of oxygen in the fuel and the absence of aromatics compounds [48, 49].

572 Regarding the DOC behavior, Figs. 20-21 and 23-24 show that the catalytic process is less
573 efficient for sugarcane biodiesel for both THC and CO emissions because the mean value of the
574 percentage decrease for both emissions is similar and always lower than those for diesel S50
575 and sugarcane diesel-farnesane. The lower oxidation of CO and THC emissions from sugarcane
576 biodiesel can be explained by taking into account that the DOC was developed to oxidate CO
577 and THC from mineral diesel fuel. Therefore, the DOC could work efficiently for fuels with similar
578 chemical composition to mineral diesel fuel, such as sugarcane diesel-farnesane, but not for
579 sugarcane biodiesel, which is a mixture of fatty acid methyl esters. This mixture, as it was
580 commented previously for CO emissions, could inhibit THC oxidation as well. Previous authors
581 [50] consider that multiple HC species in the exhaust could inhibit the oxidation process at the
582 DOC, which is another impact of the chemical composition of the fuel.

583 The experimental results obtained in the present work substantiate the above hypothesis
584 since sugarcane biodiesel showed an inhibiting effect of the CO and THC oxidation process
585 compared with diesel S50 and sugarcane diesel farnesane. This experimental observation of the
586 inhibiting effect of biodiesel at the DOC supports the recent claim of previous authors who
587 suggest that real-world fuels have an inhibiting effect of the CO and THC oxidation process [46].
588 This is the first independent analysis to support this hypothesis to the authors' knowledge.

589 *CO_2 emissions*

590 Fig. 25 shows CO_2 emissions after the DOC for the ESC test cycle. Eq. (4) and Eq. (6) were used
591 to determine the CO_2 mass flow (Fig. 25b) and specific CO_2 emissions (Fig. 25a), respectively.

592

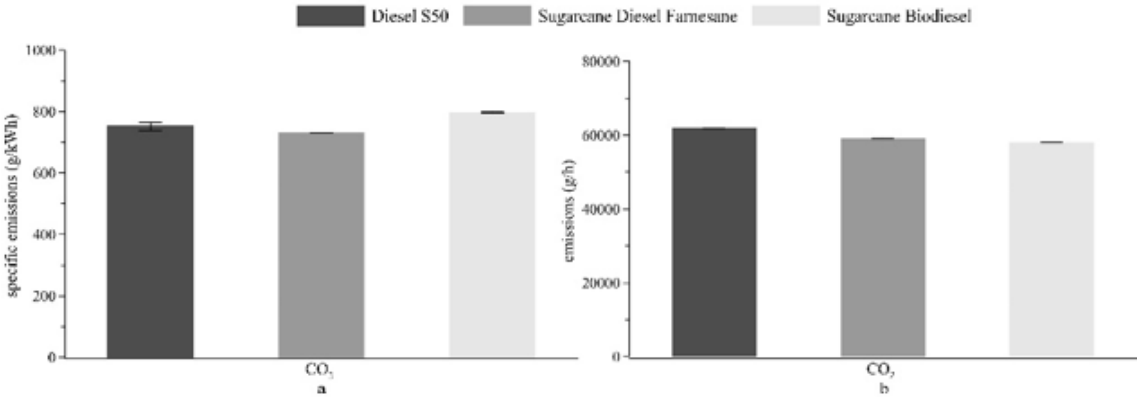

593

594 Fig. 25. Total CO_2 emissions for the ESC test after DOC: a) specific emissions b) emissions in g/h.

595 The operating regime and fuel are the primary factors influencing CO_2 emissions. Regarding
596 the fuel, the variations of the ratio H/C and the ratio O_2/C led to variations in CO_2 emissions.
597 Fuels with a low concentration of carbon have less potential to produce CO_2 emissions [45]. This
598 is one of the reasons (see Table 1) why the alternative fuels studied in the present work produce
599 lower CO_2 emissions in g/h than diesel S50 during the ESC test cycle (see Fig. 25 b). Compared
600 to the reference fuel (diesel S50), CO_2 emissions in g/h decreased by 6.44% and 4.6% for
601 sugarcane biodiesel and sugarcane diesel farnesane, respectively.

602 Fig. 26 shows that sugarcane biodiesel produced the lowest CO_2 emissions in most operating
603 regimes, while sugarcane diesel-farnesane produced lower CO_2 emissions than diesel S50 in all
604 operating regimens. Nevertheless, because of its lower engine power, specific emissions in
605 g/kW-h of sugarcane biodiesel were slightly higher (see Fig. 25a). Compared to the reference
606 fuel, emissions increased by 6.1% for sugarcane biodiesel and decreased by 2.8% for sugarcane
607 diesel farnesane.

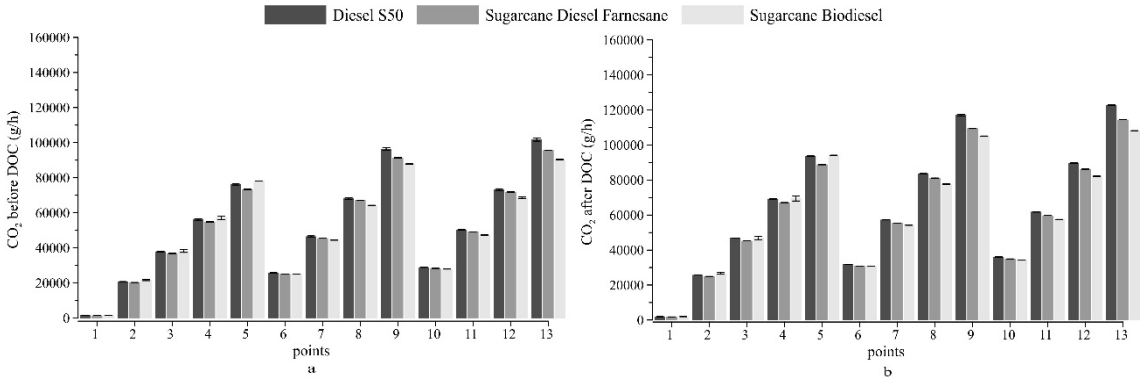

Fig. 26. CO_2 mass flow emissions g/h at each ESC mode: a) before DOC and b) after DOC.

Analyzing CO_2 emissions for the modes in which the fuels provide the same engine power (see Fig. 27), the highest emissions are observed for sugarcane biodiesel.

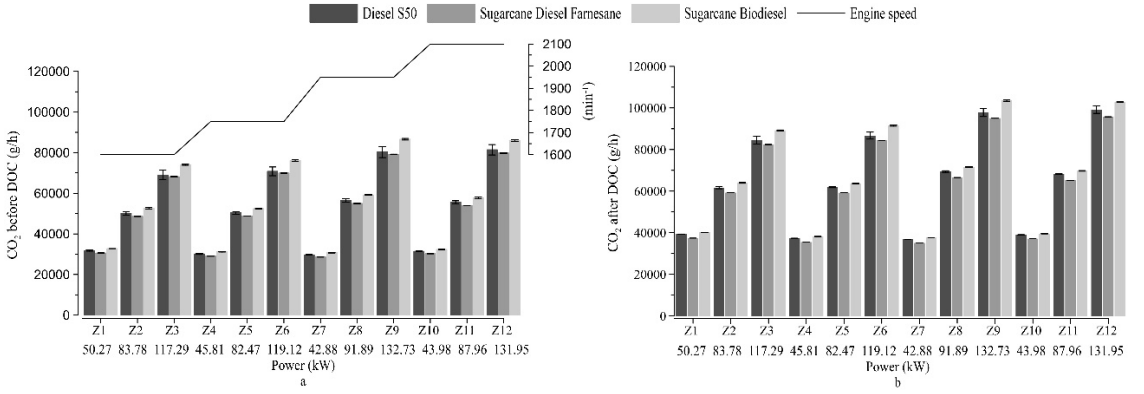

Fig. 27. CO_2 mass flow emissions (g/h) for the three fuels in each Z_i mode: a) before DOC and b) after DOC.

The low heating value of sugarcane biodiesel causes an increase in fuel consumption to maintain the same engine power, which harms biodiesel CO_2 emissions.

For the three fuels, the action of the oxidation catalyst is illustrated in Fig. 27, where an increase in CO_2 emissions between the inlet and outlet of the DOC is observed due to the CO and THC oxidation.

3.2.3. Toxicity characteristics

Previous sections provide a comparison of engine emissions among the fuels tested. This section will focus on the results for each individual fuel to examine the relationships between engine operating regimens and their toxic exhaust gases (NOx, CO, and THC). Fig. 28 portrays the toxicity characteristics as a function of engine load and speed for each tested fuel.

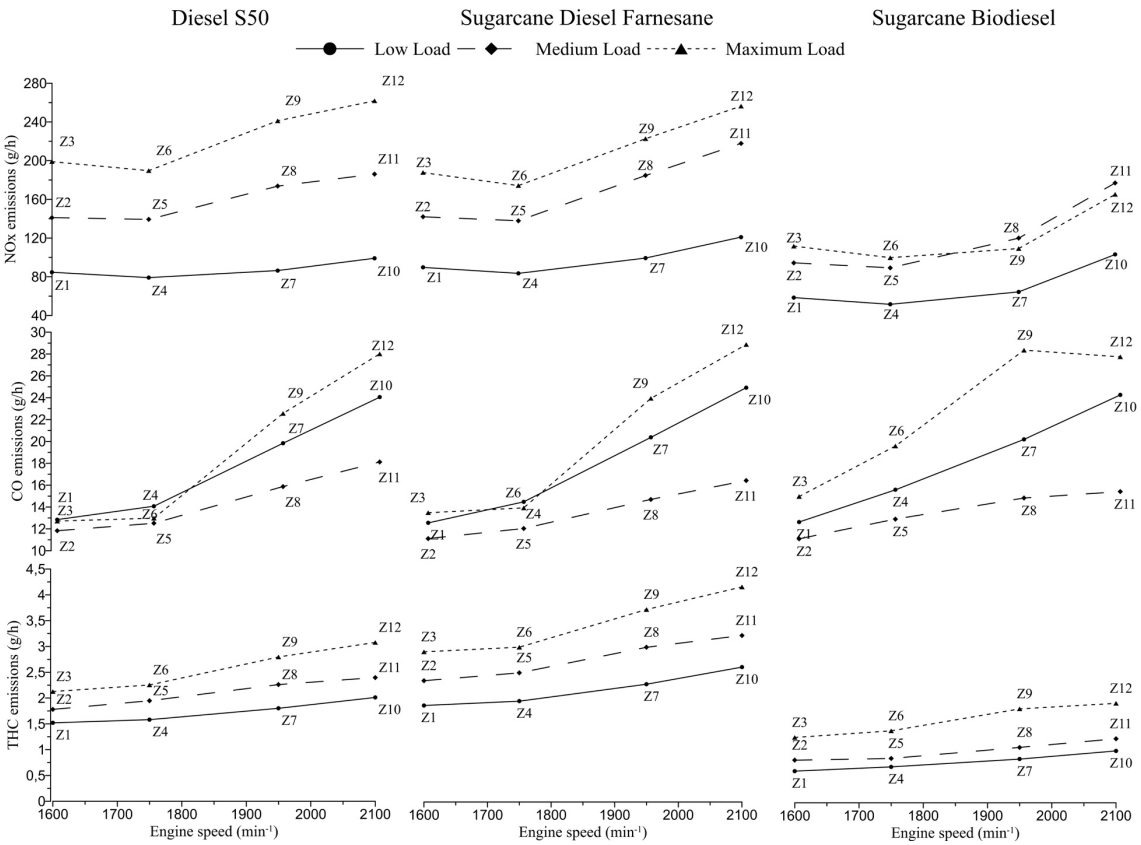

Fig. 28. Toxicity characteristics for different engine speeds and loads: low load P_e = 0.55-0.82 MPa (26%-34% load, respectively). Medium load: P_e = 1.10-1.37 MPa (52%-56% load, respectively). Maximum (high) load: P_e = 1.65-1.92 MPa (75%-81% load, respectively).

Regarding sugarcane biodiesel, it is noted that:

(i) In general, a load reduction decreases NO_x emissions due to the reduction of the combustion temperature. On the other hand, for sugarcane biodiesel, NO_x emissions at maximum load are lower than those at medium load between 1950 and 2100 min^{-1}. This is due to the fact that exhaust gas recirculation has maximum values at the operating modes Z_9 and Z_{12} (Fig. 18, Z_9_high load_m_EGR= 266.6 kg/h > Z_8_medium load_m_EGR= 165 kg/h and Z_{12}_high load_m_EGR=238.7 kg/h > Z_{11}_medium load_m_EGR= 155.5 kg/h). However, Wang et al. [51] suggest that combustion at high temperatures with reduced amounts of exhaust gas recirculation seems to improve engine performance and thermal efficiency.

(ii) In general, CO and THC emissions grow similarly with the engine speed. The high

values of m_EGR at Z_9 and Z_{12} modes lead to an increase in CO and THC emissions due to incomplete combustion.

(iii) It is noteworthy that CO emissions for all operating regimes at medium load (Z_2, Z_5, Z_8 y Z_{11}) are lower than those at low and high loads. In the case of the sugarcane biodiesel, this enhancement of the carbon oxidation at medium load can be explained by its lower LHV, which provides an optimum value of the injection duration at medium loads.

(iv) For all fuels tested, a load reduction decreases THC emissions. These emissions depend on the THC condensation on the surface of PM, and this process is influenced by the injection duration. At low loads in comparison with medium loads, injection duration decreases because injection timing is retarded. Armas, Kuen and Boehman [34] demonstrated that when injection timing of biodiesel is retarded, the mean particle diameter is reduced, which provides an increased surface area for the THC absorption and therefore, THC emissions decrease. The same analysis can be applied to the comparison between medium and maximum loads.

With respect to the sugarcane diesel-farnesane:

(i) NOx reduction is proportional to load reduction. The high LHV value of the sugarcane diesel-farnesane can explain this behavior since it leads to low fueling at low loads (Fig. 16), which is achieved by retarding the injection timing.

(ii) At low loads, the high ratio H/C and the retarded injection timing increase CO emissions due to incomplete combustion. Note that the CO curves at low and high loads are similar for low engine speeds (between 1600 and 1750 min^{-1}).

(iii) The lowest CO emissions are produced at medium load due to the optimum combination of fueling and air mass flow. During fuel injection at medium load, there is an optimum speed of the air-fuel mixing that promotes the carbon oxidation. At low loads, this speed falls below the optimum and, consequently, the

665 pressure increase in the combustion chamber is not enough to reach a complete CO
666 oxidation. Previous authors [52] claim that minimizing the increase of the rate of
667 pressure allows an extension of the combustion at low temperature, which leads to
668 decreased CO_2 formation and, consequently, an increase of CO emissions. At high
669 loads, the air-fuel mixing speed is over the optimum value and, again, this poorer
670 synchronization increases CO emissions.

671 (iv) THC curves are parallel and almost equidistant for the three loads. This is explained
672 by two behaviors: The proportional relationship between fueling and the required
673 load (Fig. 16), and the distillation process of sugarcane diesel-farnesane, which
674 occurs at a nearly constant temperature of 252 °C (see Table 1). In other words, load
675 and fueling have a linear relationship, while fuel evaporates quickly independently
676 of the load. Therefore, THC emissions are proportional to fueling and, consequently,
677 to load.

678 Finally, regarding diesel S50:

679 (i) NOx emissions increase as the load increases, following the same tendency as
680 fueling (Fig. 16). Note that, for the diesel S50, the Z_{10} Z_{11} and Z_{12} modes show similar
681 values of m_EGR (see Fig. 18), which means that m_EGR is not proportional to load,
682 moreover, the m_EGR influences the NOx emissions. These facts can explain why
683 the NOx emissions limit was exceeded. Previous studies performed in India support
684 this result; according to Pirjola et al. [53], NOx emissions from a Euro 4 diesel vehicle,
685 which includes a NO_x reducer, exceed the limit set by the regulation.

686 (ii) For all loads and low engine speeds (from 1600 to 1750 min^{-1}), CO emissions are
687 similar. Above 1750 min^{-1}, medium load is the optimum load since CO emissions
688 show the lowest values, which is related to the physical-chemical properties of the
689 diesel S50 as they promote more complete combustion at medium load.

690 (iii) Diesel S50 is a blend of many light and heavy hydrocarbons (see distillation results

691 in Table 1). Hence, it has an early evaporation (note that more than half of the fuel
692 vaporizes at 260 ^{o}C), which promotes the fuel burning in the initial stage of the
693 combustion process. This points to a proportional relationship between the
694 increase of fueling, due to an increase of load, and the increase of THC emissions.

695 For all fuels at constant load, the available combustion time is reduced by increasing engine
696 speed, so that the characteristic emissions of incomplete combustion, CO and THC, increase.
697 Regarding NOx emissions, there is an optimum at the engine speed of 1750 min^{-1}, which
698 corresponds to the optimum condition for the turbulent diffusion combustion. Above this
699 optimum value, increasing engine speed will increase NO_x emissions. Finally, as load increases,
700 there is an increase in NO_x and THC emissions. With respect to CO emissions, the lowest values
701 were obtained at medium load.

702 A noteworthy aspect regarding the originality of this work is the determination of these
703 toxicity characteristics from the ESC tests and their importance for the analysis of gaseous
704 emissions.

705 **4. Conclusions**

706 The experimental comparison of diesel S50, sugarcane diesel-farnesane and sugarcane
707 biodiesel provides results about the engine performance and corresponding exhaust emissions.
708 The primary results regarding these emissions and their relationship with engine performance
709 and fuel physicochemical properties are summarized here. These fuels were tested under the
710 European Steady Cycle (ESC), as well as under a set of Z_i modes that provide the same engine
711 power for all tested fuels.

712 An analysis of the ESC results shows that engine power differs between fuels at each
713 operating condition due to the variation in LHV, despite the fuel/air regulation performed by the
714 ECU. Regarding harmful emissions:

715 • Specific PM emissions for the three tested fuels satisfied the limit set by the regulation.
716 For the entire ESC cycle, both biofuels showed lower PM emissions than the reference

717 diesel. In particular, the low PM emissions of the diesel-farnesane are noteworthy. Its
718 low cetane number, little or no tendency to produce soot precursors, absence of
719 aromatics in its composition, and its high hydrogen content explain this fact. The lower
720 PM emissions of the sugarcane biodiesel with respect to the diesel S50 are explained by
721 the absence of aromatic compounds and the presence of oxygen in its chemical
722 composition.

723 • Specific NOx emissions of the reference diesel S50 were above the limit set by the
724 regulation. The lowest specific emissions were produced by the sugarcane biodiesel,
725 which can be explained by the ECU control over the exhaust gas recirculation and
726 fueling.

727 • Specific CO emissions after DOC of all tested fuels were well below the limit set by the
728 regulation. Nevertheless, sugarcane biodiesel showed a higher value than the other two
729 fuels. Before DOC, in most ESC operation modes and Z_i modes, lower CO emissions were
730 observed for both biofuels in comparison with the diesel S50.

731 • Specific THC emissions from sugarcane diesel-farnesane were the highest. However,
732 these emissions were well below the limit set by the regulation. Sugarcane biodiesel and
733 the reference diesel fuel provided similar results. Before DOC for both ESC and Z_i modes,
734 the sugarcane biodiesel showed lower emissions, and the diesel-farnesane higher
735 emissions, than the diesel S50.

736 • Sugarcane biodiesel inhibits the oxidation process of CO and THC emissions at the DOC.

737 Finally, for all loads (low, medium and maximum) and the three fuels tested, the optimum
738 engine speed that provided the minimum value of NOx emissions is 1750 min^{-1}, which is related
739 to favorable diffusive combustion at this engine speed. For all loads and fuels, CO and THC
740 emissions increase as engine speed increases, since the time available for combustion
741 decreases. For the three fuels tested, NO_x and THC emissions increased with the loads. This was
742 not the case of CO emissions, which reached the lowest values at medium load.

743 Future work, which includes the measurement of some parameters such as combustion
744 chamber pressure, injection pressure, and injection timing, will help support the adoption of the
745 studied biofuels in Brazil's current road transport vehicles.

746 **Acknowledgements**

747 Authors are grateful for the provision of Research Mobility Grant from the Spanish Ministry
748 of Science, Innovation and Universities (José Castillejo CAS19/00245) to Eloísa Torres-Jiménez.
749 This work was supported by MAN-Latin America, which funded the engine experimental tests
750 executed at MAHLE Metal Leve S.A., the acquisition of the biofuels from the companies Amyris
751 and LS9 in Brazil and made the engine available for the experimental tests with all the necessary
752 accessories and technical support. The authors want to thank Professor Timothy Shedd (Director
753 of Research and Development Motivair Corporation Lancaster, NY, USA) for checking the
754 spelling and grammar of this paper.

755 **References**

756 [1] Pisano G, Wagonfeld AB. Amyris Biotechnologies: Commercializing Biofuel.
757 Harvard/Dusiness/School. N9-610-031. 2010.
758 [2] Mączyńska J, Krzywonos M, Kupczyk A, Tucki K, Sikora M, Pińkowska H, Bączyk A.,
759 Wielewska, I. Production and use of biofuels for transport in Poland and Brazil–The case
760 of bioethanol. Fuel 2019;241:989-96.
761 [3] https://www.epa.gov/greenchemistry/presidential-green-chemistry-challenge-2010-
762 small-business-award [Accessed 03/25/2020].
763 [4] Pontes MAP, Machado FBC, Roberto-Neto O, de Araujo Ferrão LF. Soot precursors in
764 farnesane and n-dodecane decomposition: A computational approach. Fuel
765 2020;268:117334.
766 [5] Oßwald P, Whitside R, Schäffer J, Köhler M. An experimental flow reactor study of the
767 combustion kinetics of terpenoid jet fuel compounds: Farnesane, p-menthane and p-
768 cymene. Fuel 2017;187:43-50.

769 [6] Guilherme S. Manual do Diesel de Cana. *In: Amyris.*; 2012.

770 [7] Cachiolo AD, D'Agosto MA, Assumpção FdC, Franca LS. O impacto do uso de biodiesel e
771 diesel de cana de açúcar nos custos de uma empresa de transporte urbano de cargas.
772 Revista de Engenharia e Tecnologia 2013;5(4):Páginas 173-84.

773 [8] Desenvolvimento de Biocombustíveis Avançados para o Brasil e o Papel do PAISS para
774 Fomento de Inovação e Produção Industrial. LS9. Seminário BNDES. 07.12.2012.

775 [9] Soto F, Marques G, Torres-Jiménez E, Vieira B, Lacerda A, Armas O, Guerrero-Villar F. A
776 comparative study of performance and regulated emissions in a medium-duty diesel
777 engine fueled with sugarcane diesel-farnesane and sugarcane biodiesel-LS9. Energy
778 2019;176:392-409.

779 [10] Conconi CC, Crnkovic PM. Thermal behavior of renewable diesel from sugar cane,
780 biodiesel, fossil diesel and their blends. Fuel processing technology 2013;114:6-11.

781 [11] Crnkovic PM, Koch C, Ávila I, Mortari DA, Cordoba AM, dos Santos AM. Determination
782 of the activation energies of beef tallow and crude glycerin combustion using
783 thermogravimetry. Biomass and bioenergy 2012;44:8-16.

784 [12] Soto F, Alves M, Valdés JC, Armas O, Crnkovic P, Rodrigues G, Lacerda A, Melo L. The
785 determination of the activation energy of diesel and biodiesel fuels and the analysis of
786 engine performance and soot emissions. Fuel Processing Technology 2018;174:69-77.

787 [13] Wang H, Oehlschlaeger MA. Autoignition studies of conventional and Fischer–Tropsch
788 jet fuels. Fuel 2012;98:249-58.

789 [14] Gowdagiri S, Wang W, Oehlschlaeger MA. A shock tube ignition delay study of
790 conventional diesel fuel and hydroprocessed renewable diesel fuel from algal oil. Fuel
791 2014;128:21-9.

792 [15] Gowdagiri S, Cesari XM, Huang M, Oehlschlaeger MA. A diesel engine study of
793 conventional and alternative diesel and jet fuels: Ignition and emissions characteristics.
794 Fuel 2014;136:253-60.

795 [16] Cecrle E, Depcik C, Duncan A, Guo J, Mangus M, Peltier E, Stagg-Williams S, Zhong Y.
796 Investigation of the effects of biodiesel feedstock on the performance and emissions of
797 a single-cylinder diesel engine. Energy & Fuels 2012;26(4):2331-41.
798 [17] Millo F, Bensaid S, Fino D, Marcano SJC, Vlachos T, Debnath BK. Influence on the
799 performance and emissions of an automotive Euro 5 diesel engine fueled with F30 from
800 Farnesane. Fuel 2014;138:134-42.
801 [18] Soriano J, Garcia-Contreras R, Leiva-Candia D, Soto F. Influence on Performance and
802 Emissions of an Automotive Diesel Engine Fueled with Biodiesel and Paraffinic Fuels:
803 GTL and Biojet Fuel Farnesane. Energy & Fuels 2018;32(4):5125-33.
804 [19] Torres-Jiménez E, Armas O, Lešnik L, Cruz-Peragón F. Methodology to simulate
805 normalized testing cycles for engines and vehicles via design of experiments with low
806 number of runs. Energy Conversion and Management 2018;177:817-32.
807 [20] ABNT NBR 15634 Veículos rodoviarios automotores – Análise e determinação do gás de
808 exaustão segundo os ciclos ETC, ESC e ELR. Associação Brasileira de Normas Técnicas.
809 2012.
810 [21] ABNT NBR 1585 Veículos rodoviarios – Código de ensaios de motores – Potencia líquida
811 efectiva. Associação Brasileira de Normas Técnicas. 1996.
812 [22] https ://www.dieselnet.com/standards/cycles/esc.php. [Accessed 03/25/2020]
813 [23] Lapuerta M, Armas O, Rodriguez-Fernandez J. Effect of biodiesel fuels on diesel engine
814 emissions. Progress in energy and combustion science 2008;34(2):198-223.
815 [24] Ramirez A, Cox C. Improving on the range rule of thumb. Rose-Hulman Undergraduate
816 Mathematics Journal 2012;13(2):1.
817 [25] GUM I. Guide to the Expression of Uncertainty in Measurement, (1995), with
818 Supplement 1, Evaluation of measurement data, JCGM 101: 2008. Organization for
819 Standardization, Geneva, Switzerland 2008.
820 [26] Arkhangel'skiĭ VM. Motor vehicle engines. Mir Publishers; 1971.

821 [27] Heywood JB. Internal combustion engine fundamentals. McGraw-Hill; 1988.

822 [28] Molina SA. Influencia de los parámetros de inyección y la recirculación de gases de
823 escape sobre el proceso de combustión en un motor diesel. Valencia Barcelona:
824 Universidad Politécnica de Valencia; Reverté; 2005.

825 [29] Markatou P, Wang H, Frenklach M. A computational study of sooting limits in laminar
826 premixed flames of ethane, ethylene, and acetylene. Combustion and flame
827 1993;93(4):467-82.

828 [30] Soriano JA, Agudelo JR, López AF, Armas O. Oxidation reactivity and nanostructural
829 characterization of the soot coming from farnesane-A novel diesel fuel derived from
830 sugar cane. Carbon 2017;125:516-29.

831 [31] Tree DR, Svensson KI. Soot processes in compression ignition engines. Progress in Energy
832 and Combustion Science 2007;33(3):272-309.

833 [32] Flynn PF, Durrett RP, Hunter GL, zur Loye AO, Akinyemi OC, Dec JE, Charles KW. Diesel
834 combustion: an integrated view combining laser diagnostics, chemical kinetics, and
835 empirical validation. SAE transactions 1999:587-600.

836 [33] Song J, Alam M, BOEHMAN∗ AL. Impact of alternative fuels on soot properties and DPF
837 regeneration. Combustion Science and Technology 2007;179(9):1991-2037.

838 [34] Armas O, Yehliu K, Boehman AL. Effect of alternative fuels on exhaust emissions during
839 diesel engine operation with matched combustion phasing. Fuel 2010;89(2):438-56.

840 [35] Wu S, Zhou D, Yang W. Implementation of an efficient method of moments for
841 treatment of soot formation and oxidation processes in three-dimensional engine
842 simulations. Applied Energy 2019;254:113661.

843 [36] Armas O, Hernández JJ, Cárdenas MD. Reduction of diesel smoke opacity from vegetable
844 oil methyl esters during transient operation. Fuel 2006;85(17-18):2427-38.

[37] Lapuerta M, Herreros JM, Lyons LL, García-Contreras R, Briceño Y. Effect of the alcohol type used in the production of waste cooking oil biodiesel on diesel performance and emissions. Fuel 2008;87(15-16):3161-9.

[38] Das DD, McEnally CS, Kwan TA, Zimmerman JB, Cannella WJ, Mueller CJ, Pfefferle, L.D. Sooting tendencies of diesel fuels, jet fuels, and their surrogates in diffusion flames. Fuel 2017;197:445-58.

[39] Soltic P, Edenhauser D, Thurnheer T, Schreiber D, Sankowski A. Experimental investigation of mineral diesel fuel, GTL fuel, RME and neat soybean and rapeseed oil combustion in a heavy duty on-road engine with exhaust gas aftertreatment. Fuel 2009;88(1):1-8.

[40] Schaberg P, Botha J, Schnell M, Hermann H-O, Pelz N, Maly R. Emissions performance of GTL diesel fuel and blends with optimized engine calibrations. SAE Technical Paper; 2005.

[41] Kitano K, Sakata I, Clark R. Effects of GTL fuel properties on DI diesel combustion. SAE transactions 2005:1415-25.

[42] Gómez A, Soriano J, Armas O. Evaluation of sooting tendency of different oxygenated and paraffinic fuels blended with diesel fuel. Fuel 2016;184:536-43.

[43] Yang Y, Boehman AL, Santoro RJ. A study of jet fuel sooting tendency using the threshold sooting index (TSI) model. Combustion and Flame 2007;149(1-2):191-205.

[44] Thangaraja J, Kannan C. Effect of exhaust gas recirculation on advanced diesel combustion and alternate fuels-A review. Applied Energy 2016;180:169-84.

[45] Payri González F, Desantes Fernández JM. Motores de combustión interna alternativos. Colección Académica Editorial UPV 2011.

[46] Majumdar SS, Pihl JA, Toops TJ. Reactivity of novel high-performance fuels on commercial three-way catalysts for control of emissions from spark-ignition engines. Applied Energy 2019;255:113640.

871 [47] Bermúdez V, Ruiz S, Novella R, Soto L. Assessment of air management strategies on
872 particulate number and size distributions from a 2-stroke compression-ignition engine
873 operating with gasoline Partially Premixed Combustion concept. International Journal
874 of Engine Research 2018:1468087418802706.
875 [48] Lefort IaHJMaTA. Reduction of Low Temperature Engine Pollutants by Understanding
876 the Exhaust Species Interactions in a Diesel Oxidation Catalyst. Environmental Science
877 \& Technology 2014;48(4):2361-7.
878 [49] Fayad MAaHJMaMFJaTA. Role of Alternative Fuels on Particulate Matter (PM)
879 Characteristics and Influence of the Diesel Oxidation Catalyst. Environmental Science \&
880 Technology 2015;49(19):11967-73.
881 [50] AL-Harbi M, Hayes R, Votsmeier M, Epling WS. Competitive NO, CO and hydrocarbon
882 oxidation reactions over a diesel oxidation catalyst. The Canadian Journal of Chemical
883 Engineering 2012;90(6):1527-38.
884 [51] Wang B, Pamminger M, Wallner T. Impact of fuel and engine operating conditions on
885 efficiency of a heavy duty truck engine running compression ignition mode using energy
886 and exergy analysis. Applied Energy 2019;254:113645.
887 [52] De Simio L, Iannaccone S. Gaseous and particle emissions in low-temperature
888 combustion diesel–HCNG dual-fuel operation with double pilot injection. Applied
889 Energy 2019;253:113602.
890 [53] Pirjola L, Kuuluvainen H, Timonen H, Saarikoski S, Teinilä K, Salo L, Datta A, Simonen P,
891 Karjalainen P, Kulmala K, Rönkkö T. Potential of renewable fuel to reduce diesel exhaust
892 particle emissions. Applied Energy 2019;254:113636.
893